comptes rendus palevol

2024 • 23 • 21

A new thumb phalanx from Moula Guercy (France): description and considerations of Neandertal hand use

Jean-Luc VOISIN, Maria Giovanna BELCASTRO, Annalisa PIETROBELLI & Silvana CONDEMI

art. 23 (21) — Published on 22 August 2024
www.cr-palevol.fr

PUBLICATIONS SCIENTIFIQUES

MUSÉUM NAL HIST NATURELLE

Couverture / *Cover* :
Made from the Figures of the article.

Comptes Rendus Palevol est indexé dans / Comptes Rendus Palevol *is indexed by:*
– Cambridge Scientific Abstracts
– Current Contents® Physical
– Chemical, and Earth Sciences®
– ISI Alerting Services®
– Geoabstracts, Geobase, Georef, Inspec, Pascal
– Science Citation Index®, Science Citation Index Expanded®
– Scopus®.

Les articles ainsi que les nouveautés nomenclaturales publiés dans *Comptes Rendus Palevol* sont référencés par / *Articles and nomenclatural novelties published in* Comptes Rendus Palevol *are registered on:*
– ZooBank® (http://zoobank.org)

Comptes Rendus Palevol est une revue en flux continu publiée par les Publications scientifiques du Muséum, Paris et l'Académie des sciences, Paris
Comptes Rendus Palevol *is a fast track journal published by the Museum Science Press, Paris and the Académie des sciences, Paris*

Les Publications scientifiques du Muséum publient aussi / *The Museum Science Press also publish:*
Adansonia, ***Geodiversitas***, ***Zoosystema***, ***Anthropozoologica***, ***European Journal of Taxonomy***, ***Naturae***, ***Cryptogamie*** **sous-sections** ***Algologie***, ***Bryologie***, ***Mycologie***.

L'Académie des sciences publie aussi / *The Académie des sciences also publishes:*
Comptes Rendus Mathématique, Comptes Rendus Physique, Comptes Rendus Mécanique, Comptes Rendus Chimie, Comptes Rendus Géoscience, Comptes Rendus Biologies.

Diffusion – Publications scientifiques Muséum national d'Histoire naturelle
CP 41 – 57 rue Cuvier F-75231 Paris cedex 05 (France)
Tél. : 33 (0)1 40 79 48 05 / Fax : 33 (0)1 40 79 38 40
diff.pub@mnhn.fr / https://sciencepress.mnhn.fr

Académie des sciences, Institut de France, 23 quai de Conti, 75006 Paris.

ISSN (imprimé / *print*) : 1631-0683/ ISSN (électronique / *electronic*) : 1777-571X

A new thumb phalanx from Moula Guercy (France): description and considerations of Neandertal hand use

Jean-Luc VOISIN
ADES (anthropologie bio-culturelle, droit, éthique et santé),
Aix Marseille Université, CNRS, EFS, ADES, Faculté de Médecine, La Timone,
27 boulevard Jean Moulin, F-13385 Marseille Cedex 05 (France)
jeanlucvoisin2004@yahoo.fr (corresponding author)

Maria Giovanna BELCASTRO
Annalisa PIETROBELLI
Dipartimento di Scienze Biologiche, Geologiche e Ambientali,
Alma Mater Studiorum Università di Bologna, Via Selmi 3, 40126 Bologna (Italy)

Silvana CONDEMI
ADES (anthropologie bio-culturelle, droit, éthique et santé),
Aix Marseille Université, CNRS, EFS, ADES, Faculté de Médecine, La Timone,
27 boulevard Jean Moulin, F-13385 Marseille Cedex 05 (France)
silvana.condemi@univ-amu.fr (corresponding author)

Submitted on 23 June 2023 | Accepted on 26 April 2024 | Published on 22 August 2024

urn:lsid:zoobank.org:pub:C6B8788F-F6EB-46C8-8A01-7AC421AEAC0B

Voisin J.-L., Belcastro M. G., Pietrobelli A. & Condemi S. 2024. — A new thumb phalanx from Moula Guercy (France): description and considerations of Neandertal hand use. *Comptes Rendus Palevol* 23 (21): 293-323. https://doi.org/10.5852/cr-palevol2024v23a21

ABSTRACT
In this study we describe an adult left first pollical (thumb) proximal phalanx (I2-104) from the Baume de Moula-Guercy (Ardèche, France) and we evaluate its taxonomic status. We first describe this bone in detail, taking into account its pathology, before comparing it, through multivariate analyses, with a diverse sample of recent and fossil humans. Based on metric and morphological comparisons, we show that this phalanx belongs to a Neandertal individual who suffered from osteoarthritis. Osteoarthritis can have different origins, including overuse, degeneration, trauma and infection. Each of these possible etiologies is explored in our study. Although the cause is difficult to identify, the pathology in this individual may represent an inflammatory reaction caused by repeated and intense vibrations provoked by the high-frequency knapping of the left hand over time.

KEY WORDS
Hand,
handedness,
Tepe Hissar,
Certosa collection,
Olivier collection,
Neandertal,
phalanx.

RÉSUMÉ
Une nouvelle phalange de pouce provenant de Moula Guercy (France) : description et réflexion sur l'utilisation de la main par les Néandertaliens.
Dans cette étude, nous décrivons une première phalange proximale de pouce adulte (I2-104) provenant de la Baume de Moula-Guercy (Ardèche, France) et nous évaluons son statut taxonomique. Pour atteindre notre objectif, nous avons d'abord décrit cet os en détail, pris en compte sa pathologie, avant de le comparer, par des analyses multivariées, à un échantillon diversifié d'humains récents et fossiles. Sur base de comparaisons métriques et morphologiques, nous montrons que cette phalange appartient à un individu de Néandertal ayant souffert d'arthrose. L'arthrose peut avoir différentes origines, notamment la surutilisation, la dégénérescence, les traumatismes et les infections. Chacune de ces étiologies possibles a été explorée dans notre étude. Bien que la cause soit difficile à identifier, cette pathologie présente sur I2-104 de Moula-Guercy pourrait être due à l'âge de cet individu présentant une réaction inflammatoire causée par des vibrations répétées et intenses provoquées par la taille à haute fréquence de la main gauche.

MOTS CLÉS
Main,
manipulation,
Tepe Hissar,
collection Certosa,
collection Olivier,
Néandertal,
phalange.

INTRODUCTION

The Baume de Moula-Guercy (Moula-Guercy cave) lies on a calcareous cliff 80 m above the west bank of the Rhone River close to the village of Soyons, 10 km south of Valence, Ardèche, France (Fig. 1). It was discovered in 1970 or 1972 by M. Moula (Crégut-Bonnoure *et al.* 2010; Hlusko *et al.* 2013). The site is composed of six cavities, the majority of which were occupied in the Middle Pleistocene. Moula-Guercy cave was first excavated between 1975 and 1982 by P. Paven, with later excavations conducted by A. Defleur between 1993 and 1999, following an initial survey undertaken in 1991 (Willmes *et al.* 2016). Crégut-Bonnoure *et al.* (2010) mistakenly reported that the A. Defleur excavations were made between 1992 and 2001, which does not correspond to the excavation report held at the Soyons Museum.

Stratigraphic, geological (Saos *et al.* 2014) and biochronological analyses (Defleur *et al.* 2001) identified the subdivision of the filling into three main climatic phases corresponding to MIS 6 to 4. MIS 6 layers have only been minimally explored. MIS 5 is represented by layers XV to XI and MIS 5e by layers XV and XIV (Willmes *et al.* 2016). Layer XV is the most important level of the cave, with a thickness of about 40/50 cm covering an area of about 30 to 40 m², of which only a small part has been excavated. The megafauna of layer XV includes red deer (*Cervus elaphus* Linnaeus, 1758), giant deer (*Megaloceros giganteus* Blumenbach, 1799), straight-tusked elephant (*Palaeoloxodon antiquus* Falconer & Cautley, 1847), and Asiatic black bear (*Ursus thibetanus* Cuvier, 1823), all typical of an interglacial phase (Valensi *et al.* 2012). Levels younger than layer XV have been almost completely destroyed by previous excavations.

Charcoal remains collected on the living floor of the layer XV (Defleur *et al.* 2001) have been identified with several species, including deciduous oak (*Quercus* sp.), beech (*Fagus sylvatica* Linné, 1753), elm (*Ulmus* sp.), Scots pine (*Pinus type silvestris* Linné, 1753), common juniper (*Juniperus communis* Linné, 1753), buckthorn (*Ramnus saxatilis* Jacq, 1762), blackthorn (*Prunus spinosa* Linné, 1753), ivy (*Hedera helix* Linné, 1753), and the common wild rose (*Rosa* sp.). These species are typical of temperate zone deciduous forests similar to those of the present day. Remains of rodents, reptiles, and amphibians confirm the temperate character of the abundant mammalian fauna (Defleur *et al.* 2001; Valensi *et al.* 2012).

From analysis of faunal remains, Valensi *et al.* (2012) concluded that layer XV represents a short-term occupation of the cave sometime between the end of the summer and the beginning of the autumn season. Paleoenvironmental evidence has confirmed that these occupations occurred during the Eemian period (Defleur *et al.* 2001). Additionally, recent dating by several methods (AMS radiocarbon dating on three faunal bones, 40Ar/39Ar dating on sanidine grains, U-series and ESR dating carried out on 14 faunal teeth and three human teeth) yielded an age of 120-130 ka (Willmes *et al.* 2016), again in accordance with both the palaeoecological and biochronological data provided by both large and small vertebrate faunal remains. At that time, in Western Europe, there was only one well-known human population with a set of particular morphological and genetic characteristics: the Neandertals. The origin and development of Neandertals can be followed in Europe from 300 000 years ago (end of MIS 9). They expanded towards Asia (the Levant and in the Altai region) around 100 000 years ago (MIS 5). They disappeared following the expansion from Africa of *Homo sapiens* Linnaeus, 1758. In Europe, the first occurrence of *Homo sapiens* is unanimously accepted to have taken place around 42 000 years ago (MIS 3, Higham *et al.* 2014), although a recent study from one site in southern France suggests a possible arrival as early as 54 000 years ago (beginning of MIS 3, Slimak *et al.* 2022).

FIG. 1. — Map of France showing the location of the Baume de Moula-Guercy. Credits: IGN Open Source.

TABLE 1. — Hand remains from Moula-Guercy with their associated stratigraphic layers. *, Noted in layer XIV (Mersey *et al.* 2013b); **, noted in layer XVI (Mersey *et al.* 2013b); ***, noted off stratigraphy (Mersey *et al.* 2013b).

Specimen number	Layer	Element	Authors
I2-104	XV	Proximal thumb left phalanx	This study
F1-461	XV	Left capitates	Mersey *et al.* 2013b
G2-648	XV	Left 2nd metacarpal	Mersey *et al.* 2013b
D3-768	XV	Left 3rd metacarpal	Mersey *et al.* 2013b
E1-123	XV*	Proximal hand phalanx	Mersey *et al.* 2013b
D4-48	XV**	Proximal hand phalanx	Mersey *et al.* 2013b
D1-160	XV	Proximal hand phalanx	Mersey *et al.* 2013b
G1-154	XV	Intermediate hand phalanx	Mersey *et al.* 2013b
K0-HNN1	XV***	Distal hand phalanx	Mersey *et al.* 2013b
H1-HNN2	XV	Distal hand phalanx	Mersey *et al.* 2013b
F1-359	XV	Distal hand phalanx	Mersey *et al.* 2013b

In the series of excavations at Moula-Guercy cave from 1993-1999, hominin remains, Mousterian artifacts, and faunal materials were recovered from the site (Defleur 1995; Defleur & Desclaux 1997; Defleur *et al.* 1998, 1999, 2001). All Neandertal fossils derive from level XV, although initially some of the remains were erroneously assigned to the upper part of layer XIV or the lower part of layer XVI (Mersey *et al.* 2013a, b). More than one hundred hominin specimens were excavated and have previously been described as Neandertal, representing at least six individuals, although the remains are not close to each other and are mixed with other faunal bones (Defleur 1995; Defleur *et al.* 1998, 1999; Hlusko *et al.* 2013; Mersey *et al.* 2013a, b; Richards *et al.* 2021, 2022). However, manual and pedal remains have been attributed to Neandertal only on the basis of their stratigraphic position, and recent discoveries in the area show that modern humans could have arrived much earlier than previously thought (Harvati *et al.* 2019; Slimak *et al.* 2022). Thus it is interesting to evaluate the variability of phalanges in Neandertals from MIS 5 compared to those fossils available in Europe and those from modern humans.

TABLE 2. — Dating and geographical position of the Upper Paleolithic and Middle Paleolithic remains. See also Appendix 1.

Remains	Date	Country	Sources
Upper Paleolithic and Taforalt			
Abri Pataud	39600-38900 BP	France	Higham *et al.* 2011
Chancelade	19500-18000 BP	France	Barshay-Szmidt *et al.* 2016
Cro-Magnon	28000 BP	France	Henry-Gambier 2002
Dame du Cavillon	24000 BP	France	Valladas *et al.* 2016
Dolni Vestonice 14 and 16	27000 to 25000 BP	Czech Republic	Svoboda 2006a
Nazlet Khater 2	38000 +/- 6000	Egypt	Crevecoeur & Villotte 2006
Predmost IV	Around 26500 BP	Czech Republic	Djindjian *et al.* 1999; Svoboda 2006b
Qafzeh 9	92000 BP	Israel	Valladas & Valladas 1991
Saint-Germain-la-Rivière	16000-14000 BP	France	Gambier *et al.* 2000
Šandalja II	12320 +/- 100 BP	Croatia	Janković *et al.* 2012
Sunghir 1 and 3	28000 BP	Russia	Trinkaus *et al.* 2014a
Skhul IV	100000 to 130000 BP	Israel	Mercier *et al.* 1993; Grün *et al.* 2005
Taforalt	11900 BP	Morocco	Roche 1959, 1976, but see also Bouzouggar *et al.* 2008
Middle Paleolithic Neandertal			
Hortus (Neandertal)	MIS 3 (57000 BP)	France	de Lumley 1973
Kebara 2 (Neandertal)	64000 to 59000	Israel	Valladas & Valladas 1991
Krapina (Neandertal)	130000 +/- 10000	Croatia	Rink *et al.* 1995
La Ferrassie (Neandertal)	45000 to 43000 BP	France	Guérin *et al.* 2015
Moula Guercy (Neandertal)	120000 to 130000 BP	France	Willmes *et al.* 2016
Neander (Neandertal)	40000 BP	Germany	Schmitz *et al.* 2002
Shanidar (Neandertal) 4 and 6	60000 BP	Iraq	Cowgill *et al.* 2007
Shanidar (Neandertal) 5	40000 to 50000 BP	Iraq	Cowgill *et al.* 2007
Spy 2 (Neandertal)	36000 BP	Belgium	Semal *et al.* 2009
Tabun (Neandertal)	122000 +/- 16000	Israel	Grün & Stringer 2000; Mercier & Valadas 2003

The hominin remains display numerous cut marks and other evidence of processing and likely butchery (Defleur *et al.* 1993, 1999), leading Defleur & Desclaux (2019) to suggest nutritional cannibalism, although this hypothesis has been debated (Defleur *et al.* 2020; Slimak & Nicholson 2020). Because of marrow extraction and presumably consumption, all Neandertal remains from Moula-Guercy are highly fragmentary, except the nearly marrowless hand and foot bones, which are intact. The Moula-Guercy Neandertal collection includes ten hand bones, namely carpals, metacarpals, and phalanges (Table 1).

Because the thumb can oppose itself to any other finger, it allows a strong and precise grip. Indeed, hand grasping abilities characteristic of *Homo sapiens* are a relatively strong power grip and a very efficient pad-to-pad precision grip (Richmond *et al.* 2016). The efficiency of this last grip does not exist in any other primate, except perhaps the Gelada baboons (Richmond *et al.* 2016). The efficiency of the precision grip in humans is due to an association of anatomical characteristics of the hand itself, the upper limb and the nervous system. Among the characteristics of the hand, the ratio of the length of the thumb to the other phalanges is an important one. Modern humans are characterized by long thumbs in relation to the other fingers (Richmond *et al.* 2016). These bony characteristics are associated with a particular muscular arrangement. Compared to other great apes, two additional muscles (the *flexor pollicis longus* and the *extensor pollicis brevis*) insert on the thumb in humans (Diogo *et al.* 2012; Lemelin & Diogo 2016) and the thumb muscles are more developed in humans than in other apes (Tuttle 1969).

The Neandertal hand, and more precisely the thumb, follows the same pattern of digital proportions as in modern humans, but the pollical proximal phalanx is relatively shorter and the distal pollical phalanx is relatively longer than in modern humans (Musgrave 1971). In order to identify their particular features in regard to other human groups, above all to modern humans, Neandertal hand bones have been extensively studied through primary description, as well as through the interpretive lens of both mechanical and functional analyses (i.e., Musgrave 1971, 1973; Vlček 1975; Heim 1983; Orban & Leguebe 1990; Trinkaus & Villemeur 1991; Trinkaus *et al.* 1991, 2014b; Villemeur 1992, 1994; Niewoehner *et al.* 1997, 2003; Mersey *et al.* 2013b; Karakostis *et al.* 2018; Bardo *et al.* 2020). Although there is still debate about the accuracy of Neandertal hand ability, there seems to be consensus that Neandertals may have had a stronger power grip (for a definition and a description of each type of grip see Fragaszy & Crast (2016)), especially the transverse grip, than modern humans, but that both modern humans and Neandertals had a similar precision grip (i.e., Trinkaus & Villemeur 1991; Villemeur 1992; Niewoehner 2006; and references therein; Karakostis *et al.* 2018; Bardo *et al.* 2020). The aim of this work is to describe a new proximal Neandertal pollical phalanx (I2-104) from MIS 5 and see if it corresponds to neandertal variation and include it in the broad aspect of Neandertal hand skills.

This left pollical proximal phalanx (I2-104) was discovered at la Baume de Moula-Guercy during the excavation in the summer of 1998 in zone number 2, which comprises lines D to I/ and 0 to 5 (partially) within layer XV (Defleur 2015). It was recently identified as human during sorting of faunal remains.

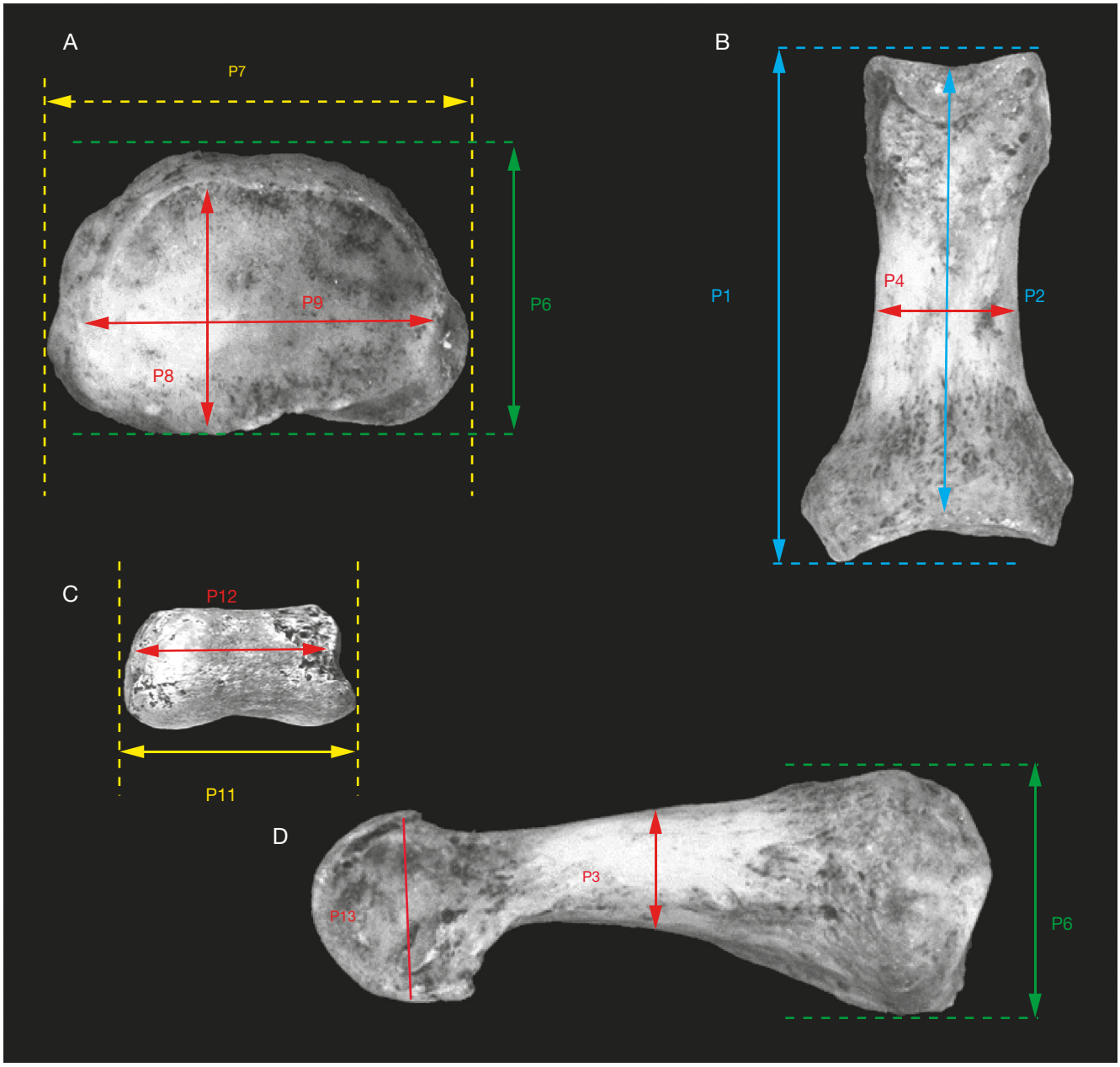

FIG. 2. — Phalanx measurements, see also Table 4; P5 cannot be shown on picture; P10 and P13 can be identical, depending on morphology: **A**, proximal view; **B**, superior view; **C**, distal view; **D**, lateral view.

MATERIAL AND METHODS

MATERIAL

Specimen I2-104 is a left pollical proximal phalanx located in the Neandertal fossil collection of the musée archéologique de Soyons (Ardèche, France). The comparative data for other pollical proximal phalanges from Neandertals and upper Paleolithic individuals (Table 2; Appendix 1) come either from the literature or from Erik Trinkaus' personal dataset, except for the Taforalt remains, which were measured by us. Our comparative data from modern *Homo sapiens* were taken for this study from three collections of adult individuals of known sex and age: the Georges Olivier collection (specimens from French hospitals, middle 20th century), the Musée de l'Homme (Paris, France), the Certosa collection (specimens from 19th and early 20th century cemeteries) of the University of Bologna (Bologna, Italy) (Facchini *et al.* 2006; Belcastro *et al.* 2017), and from the Tepe Hissar (Iran) archeological collection housed at the Penn Museum (University of Pennsylvania, Philadelphia, United States). The Tepe Hissar site covers a period from 5000 years to 2000 years BC, i.e., a period covering the Chalcolithic and much of the Bronze Age (Gürsan-Salzmann 2016). Thus, the human comparative material includes a total of 167 pollical proximal phalanges (Table 3). All the raw data are presented in an Excel table as a supplementary file (Appendix 1). The Upper Paleolithic

TABLE 3. — Number of individuals from each human group, on each side and by sex

Human groups	Total number	Left phalanx	Right phalanx	Male	Female	Unknown sexe
Neandertal	12 (without I2-104)	7	5	7	3	2
Upper Paleolithic (without Taforalt)	9	3	6	6	3	0
Taforalt	25	Not lateralized	Not lateralized	Not sexed	Not sexed	0
Tepe Hissar	24	Not lateralized	Not lateralized	Not sexed	Not sexed	0
Olivier collection	36	18	18	20	16	0
Certosa collection	59	29	30	30	29	0

TABLE 4. — Measurements taken on the first phalanx of the thumb; in the main text, phalanx height and phalanx width are grouped in the expression mid-shaft diameters. See also Figure 3.

Variables		
Localization	Code: Name	Description
Diaphysis variables	P1: Maximum length	Maximal bone length
	P2: Morphological length or articular length	Length between the center of the proximal joint and the center of the trochlea of the head
	P3: Phalanx height or Phalanx thickness	Length, at the middle, between the dorsal and the palmar surfaces of the bone
	P4: Phalanx width	Phalanx width, at the middle, taken perpendicular to the thickness
	P5: Phalanx circumference	Phalanx circumference taken at the middle of the bone
Proximal epiphysis variables	P6: Maximum height of the proximal epiphysis	The greatest dimension between the dorsal and the palmar surfaces at the proximal epiphysis
	P7: Maximum width of the proximal epiphysis	The greatest dimension, according to the latero-medial axis at the proximal epiphysis
	P8: Proximal articular height	Maximum length of the proximal joint in the dorso-palmar axis
	P9: Proximal articular width	The greatest dimension of the proximal articulation in the latero-medial axis
Distal epiphysis variables	P10: Maximum height of the distal epiphysis	Maximum length of the distal joint in the dorso-palmar axis
	P11: Maximum width of the distal epiphysis	The greatest dimension of the distal epiphysis in the latero-medial axis
	P12: Distal articular width	The greatest dimension of the distal articulation in the latero-medial axis
	P13: Distal articular height	The greatest dimension of the distal articulation in the dorso-palmar axis

sample does not include the Taforalt remains because they belong to a non-European endogamous population (Ferembach 1960, 1963; Ferembach *et al.* 1962), although some genetic links with European Mediterranean populations exist (Kéfi *et al.* 2005).

METHODS

Anthropometric analysis forms the core of the assessment of this Moula-Guercy proximal phalanx. Measurements were made with a sliding caliper (Fischer Darex 150 mm – 6 inch) and the values are presented in millimeters. Thirteen measures were defined (Table 4; Fig. 2) and correspond to those established by Trinkaus & Villemeur (1991), Villemeur (1994) and Trinkaus (1983), in order to facilitate comparison with other fossil samples.

Comparative measurements from both Neandertal and Upper Paleolithic modern human phalanges are taken from the literature. However, the vast majority of these publications present only one length measurement (either the maximum length, named variable P1, or the morphological length, named variable P2) and it is therefore difficult to make comparisons between fossil phalanges. Thus, we established a regression line derived from complete datasets of modern humans (Olivier collection, Certosa collection and Tepe Hissar) that allows us to estimate the value of one measurement when the other is known (Fig. 3; see also Appendices 2-4). The regression line has been computed with the ordinary least squares (OLS) algorithm, which is the best method when the goal is only to predict one variable using the other (Hammer & Harper 2023). Because it is impossible at first sight to differentiate the pollical phalanx of Neandertal from that of modern humans, because there are no obvious differences between them (Musgrave 1971, 1973), it is possible to establish a regression line between the maximum length and the morphological length by using only present-day *Homo sapiens* to estimate the length of Neandertal first pollical phalanges.

Because data used here come from our own measurements as well as from the literature, an inter-observer repeatability assessment was performed (see Appendices 5; 6) using the technical error of measurement (TEM) (Perini *et al.* 2005; Langley *et al.* 2018). The result shows that the inter-observer error is very low, and thus acceptable.

The statistical processing was carried out using PAST® software, version 4.03 (Hammer *et al.* 2001; Hammer & Harper 2006). The principal component analysis (PCA) relies on a variance-covariance matrix, regardless of the fact

A

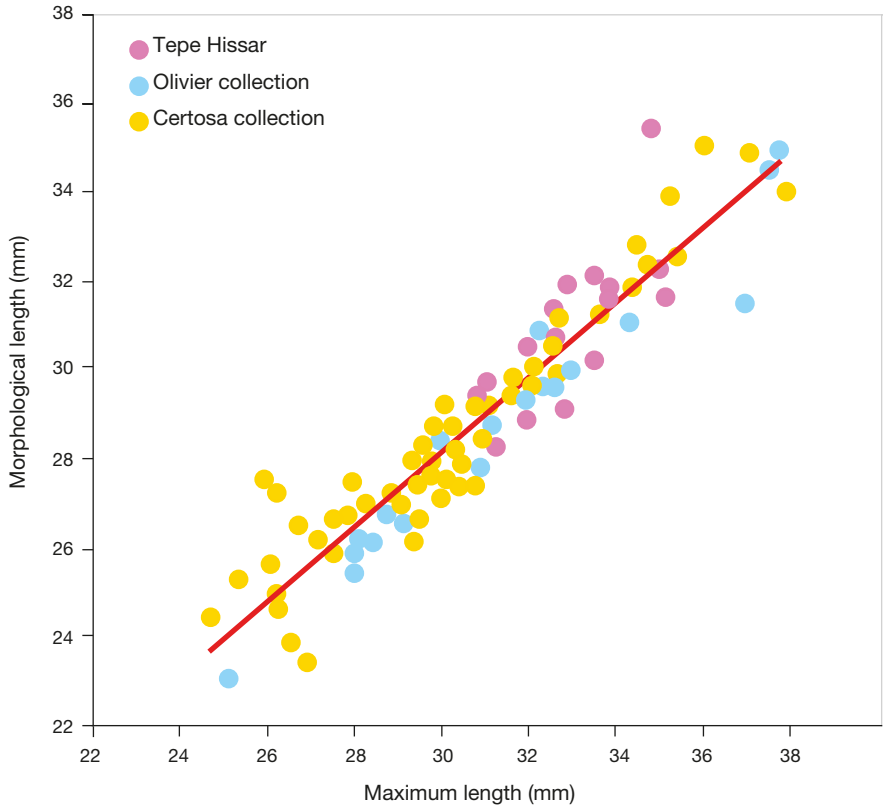

95% bootstrapped confidence intervals (N = 1999)	
Slope a	(0.7676 – 0.91383)
Intercept b	(0.70548 – 5.2117)

Ordinary least squares regression	
Slope a	0.84018
Intercept b	2.9494
Std. error a	0.027121
Std. error b	0.84053

Correlation	
r	0.9441
r^2	0.89134
t	30.979
P (uncorr.)	$3.1782*10^{-58}$
Permutation P	0.0001

B

95% bootstrapped confidence intervals (N = 1999)	
Slope a	(0.81406 – 1.151)
Intercept b	(–2.4053 – 7.467)

Ordinary least squares regression	
Slope a	0.96844
Intercept b	2.9624
Std. error a	0.042405
Std. error b	1.2267

Correlation	
r	0.90305
r^2	0.8155
t	22.838
P (uncorr.)	$4.0025*10^{-45}$
Permutation P	0.0001

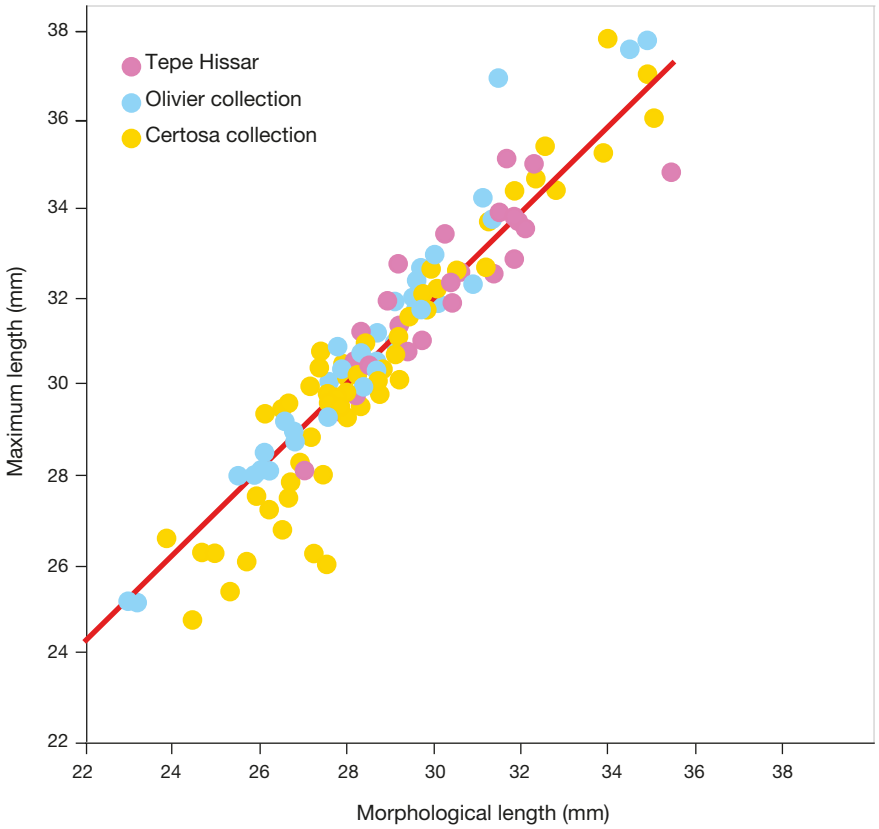

Fig. 3. — Linear regression, with the statistical outputs, between maximum and morphological lengths established from three collections of adult individuals (George Olivier, Certosa and Tepe Hissar): **A**, Y = 0.84018x + 2.9494; **B**, Y = 0.96844x + 2.9624.

TABLE 5. — Metric characteristics (in mm) of the Neandertal phalanx I2-104 of the Baume Moula-Guercy.

Reference number	I2-104
Laterality	Right
Shaft	
P1: Maximum length	26.0
P2: Morphological length	23.9
P3 Phalanx thickness	7.5
P4: Phalanx width	11.9
P5: Phalanx circumference	32.0
Proximal Epiphysis	
P6: Maximum height of the proximal epiphysis	11.2
P7: Maximum width of the proximal epiphysis	14.7
P8: Proximal articular height-	10.0
P9 : Proximal articular width	14.7
Distal Epiphysis	
P10: Maximum height of the distal epiphysis	7.5
P11: Maximum width of the distal epiphysis.	14.4
P12: Distal articular width	14.5
P13: Distal articular height	7.5

that measurements have distinct ranges, because size has its own interest. However, to avoid size effect we also ran a PCA relying on a correlation matrix. Moreover, missing data (other than those affecting variables P1, the maximum length, and P2, the morphological length, which were determined using the regression line) from the PCAs was replaced by statistically derived data obtained by iteration using the methods outlined in Hammer & Harper (2006, 2023), thus producing replacement data sets more accurately than by reliance on average values. The iterative imputation first replaces missing values by their column average and then runs an initial PCA, which is used to compute regression values for the missing data. The procedure is iterated until convergence (Hammer & Harper 2023).

Regardless of the technique used for data replacement, it is always a major factor of bias in PCA. Thus, we have also run a PCA with only the three modern human collections (Tepe Hissar, Olivier and Certosa), which is in the Appendices 1; 6-8, to determine whether or not missing data replacement produces an important bias. The number of principal components to plot, for each PCA, was decided by using the scree plot technique, proposed in PAST software.

ABBREVIATIONS

OLS ordinary least squares;
PCA principal component analysis;
TEM technical error of measurement.

RESULTS

MORPHOLOGY

I2-104 is a pollical proximal phalanx (hand ray digit 1) of an adult left hand (Fig. 4; Condemi *et al.* 2023).

I2-104 has no peculiar morphological characters and it is well preserved, but shows a large asymmetric eburnation on the palmar surface of the bone and an extensively developed osteophyte on the lateral surface (Condemi *et al.* 2023). This pathology has been described recently and could be osteoarthritis reflecting effects of genetic makeup, overuse, and aging (Condemi *et al.* 2023).

METRIC ANALYSIS

In most metric analyses, the I2-104 values (Table 5) are close to the Neandertal median values (Figs 5; 6), in particular, the maximum and morphological lengths (variables P1 and P2) of I2-104. These two latter variables are also within the lower end of variation of modern humans. Compared to the sample of Upper Paleolithic specimens, the maximum length of I2-104 is smaller, while its morphological length is within the range of variation of these early modern human specimens. This result is consistent with previous studies that describe a rather short Neandertal pollical proximal phalanx (Musgrave 1971). It is interesting to note however that, in comparison to any other modern group used in this analysis, both maximum and morphological length show a much greater variation in Neandertals than in any other human group studied here (Fig. 5).

The midshaft width (variable P4) dimension of the I2-104 phalanx is outside the range of variation in modern humans (Fig. 5) and is similar to the robust phalanx width of the Neandertal Regourdou 1. On the other hand, the phalanx height (or variable P3) in the middle of I2-104 is not exceptional but remains in the upper half of Neandertal variability (Fig. 5). The large width (or variable P4 in Table 4) of this phalanx explains, at least in part, the exceptionally high value for a Neandertal of its circumference in the middle. It is interesting to note that the human group with the largest perimeter variation in the sample present in our study is not the Neandertal group but the male population of the Certosa collection. This latter collection has extreme values similar to those of Neandertal, but lower median ones.

The great Neandertal variability according to different variables (such as maximum and morphological lengths, phalanx height, etc.) could be explained by the fact that: 1) in this fossil population, both female and male individuals have been mixed; and 2) the remains are not contemporary and not geographically close (i.e., they do not belong to the same biological population).

MULTIVARIATE ANALYSIS

The PCA is used here purely as an exploratory tool, although all conditions required to run a PCA are fulfilled (see Appendix 6). Asymmetry is relatively limited in the linear dimensions of the proximal pollical phalanx, thus allowing bones from different sides to be used in the same PCA (Karakostis *et al.* 2017; and see also Appendices 1; 9-11). Moreover, the effect of missing data does not greatly change the PCA, since most specimens are complete or nearly complete (Appendices 1; 6-8). Similarly, PCAs relying on a variance-covariance matrix and those relying on correlation matrix do not show important differences (Figs 7; 8; Table 6; Appendices 1; 6; 12-14). The loading of some variables on the PCA, based on the correlation matrix, decreased

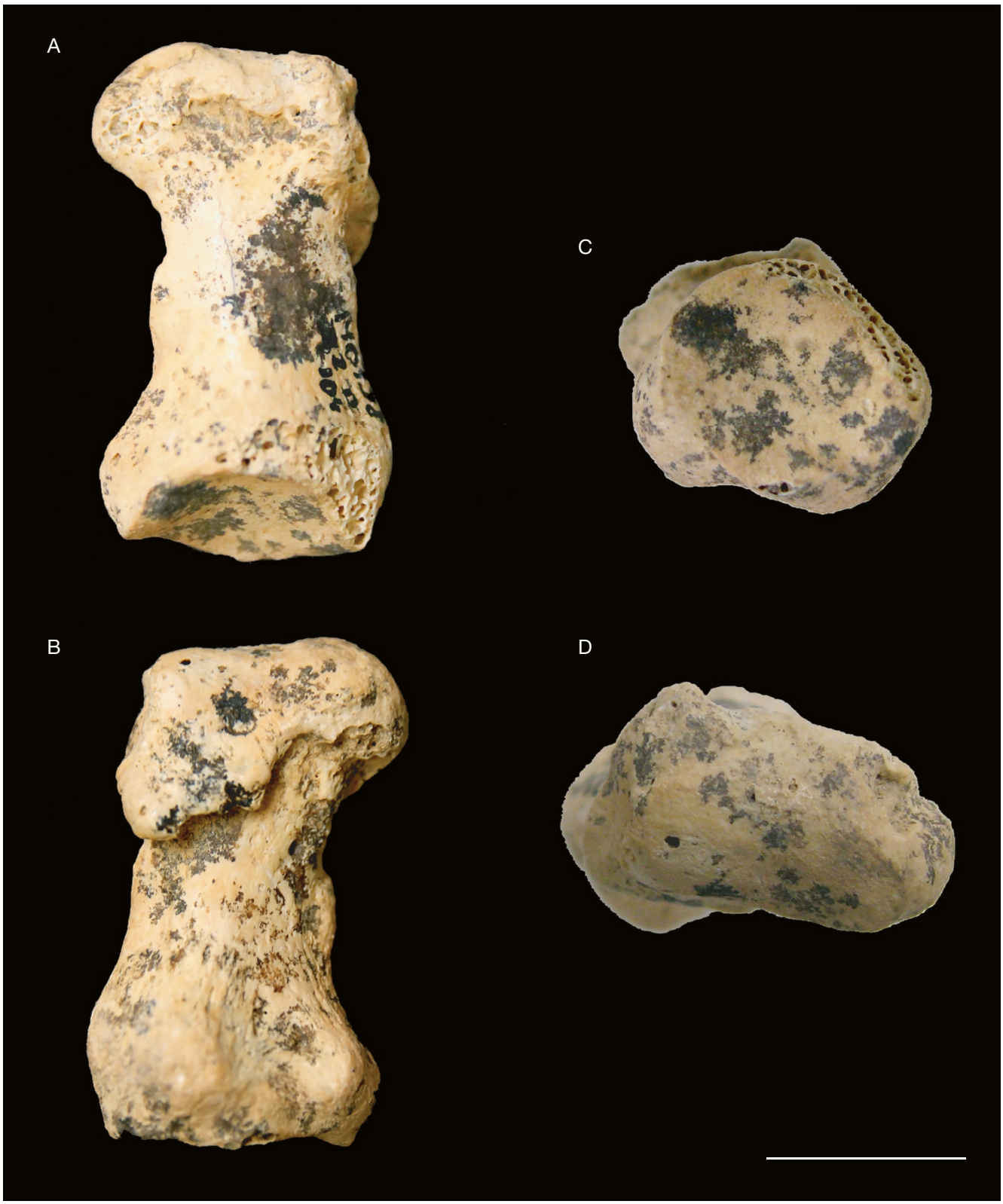

Fig. 4. — Photographs of the pollical proximal phalanx of the Moula-Guercy (I2-104): **A**, dorsal view; **B**, palmar view; **C**, proximal view, **D**, distal view. Scale bar: 1 cm.

because of loss of size effect, but the loading distribution of the variables along axes did not change outstandingly (Figs 7; 8; Table 6; Appendices 1; 6; 12-14).

Very few individuals of the European Upper Paleolithic are sufficiently complete to be used in the PCA and are all encompassed within the variability of the sample from the

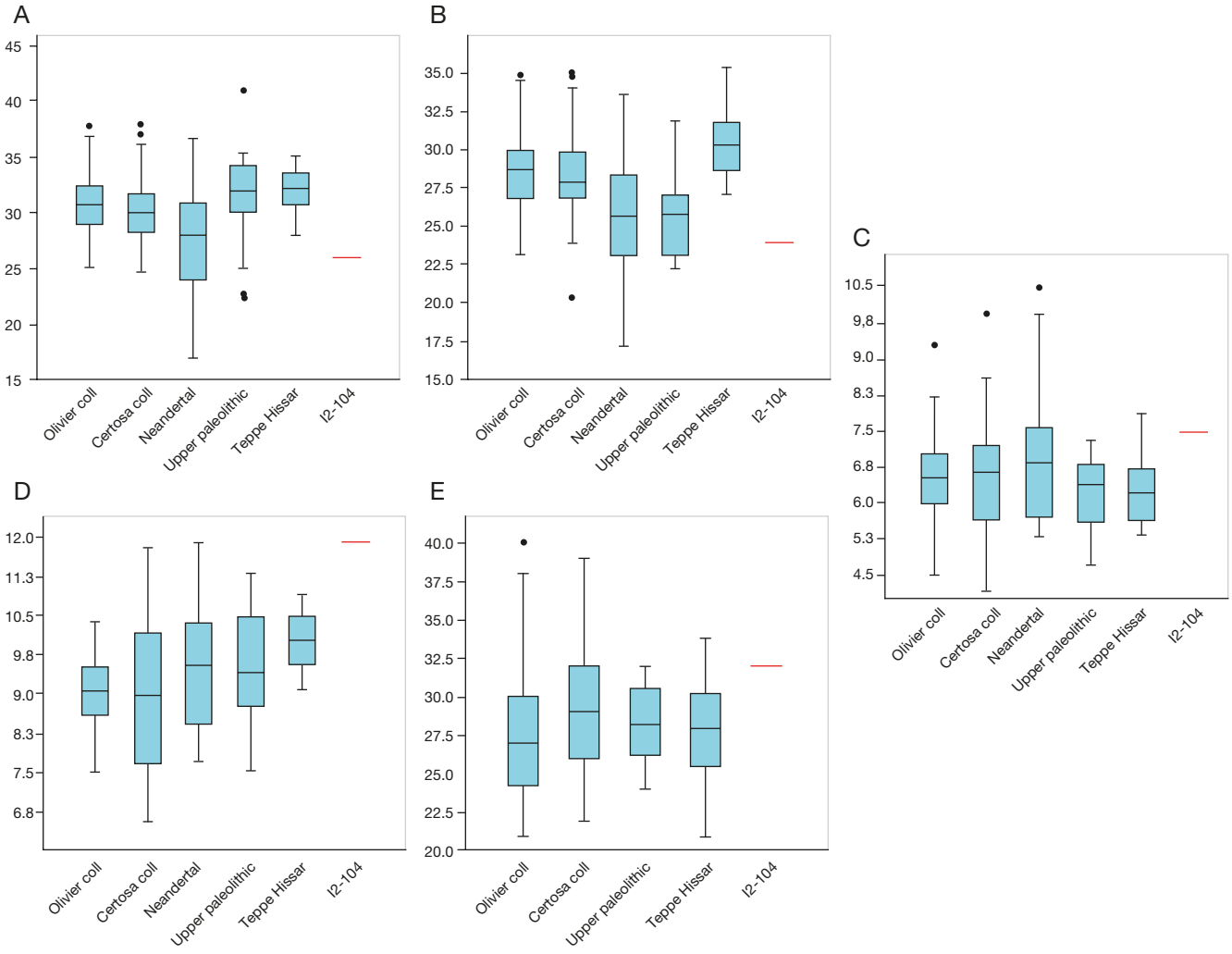

FIG. 5. — Box plot for the five diaphysis variables (in mm) describing phalanges (variables P1, P2, P3, P4 and P5): **A**, P1, maximum length; **B**, P2, morphological length; **C**, P3, phalanx height; **D**, P4, phalanx width; **E**, P5, phalanx circumference.

Olivier and Taforalt collections. The Tepe Hissar Iron Age sample from Iran is very distinct from all other modern and Neandertal populations, according to the second component. This component is positively correlated with the dimensions of the distal end (respectively variables P10, P11, P12 and P13) of the proximal phalanx and negatively with the dimensions of the proximal end (respectively variables P6, P7, P8 and P9). In other words, the Tepe Hissar sample is distinguished by a larger distal end than other populations and smaller proximal extremities (Figs 7; 8; Table 6). In contrast, the first component is positively correlated to morphological and maximum lengths and to the circumference at mid-shaft (respectively variable P1, P2 and P3). Thus, specimens that fall within the left side range of the PCA, are shorter and more gracile.

Data derived from Neandertal specimens are all included within the variability of more recent populations as well as of all the Upper Paleolithic specimens (European and Taforalt samples) (Figs 7; 8; see also Appendices 1; 6; 15-17), including the I2-104 phalanx. In other words, the Neandertal pollical proximal phalanx does not display important metric differences from modern humans. Thus, the classical description of Neandertal phalanges as characterized by broader proximal and distal joints in comparison to those of modern humans is not applicable to the pollical proximal phalanx as Musgrave (1973) noted previously. Hence, the I2-104 phalanx does not differ from other Neandertal pollical proximal phalanges and fits absolutely within Neandertal and modern human variabilities, more specifically within those from the Certosa collection. This demonstrates that Neandertal variations in pollical proximal phalanx morphology and dimensions are consistent across time and over geographic distribution, e.g. La Ferrassie 1 (France) dated to 45 to 43 ka (Guérin *et al.* 2015) and Kebara 2 (Israel) dated to 64 to 59 ka (Valladas & Valladas 1991). On the contrary, Upper Paleolithic specimens also range from a broad geographic and time distribution but tend to be more heterogeneous than Neandertals (Figs 7; 8; Table 6; Appendices 1; 6; 18; 19). This is confirmed by the Taforalt distribution, which is similar to other collections. Furthermore, the greatest variation of Tepe Hissar materials should be correlated to the greatest amount of time covered by this site (from Period 1 to Period 3; see Gürsan-Salzmann 2016).

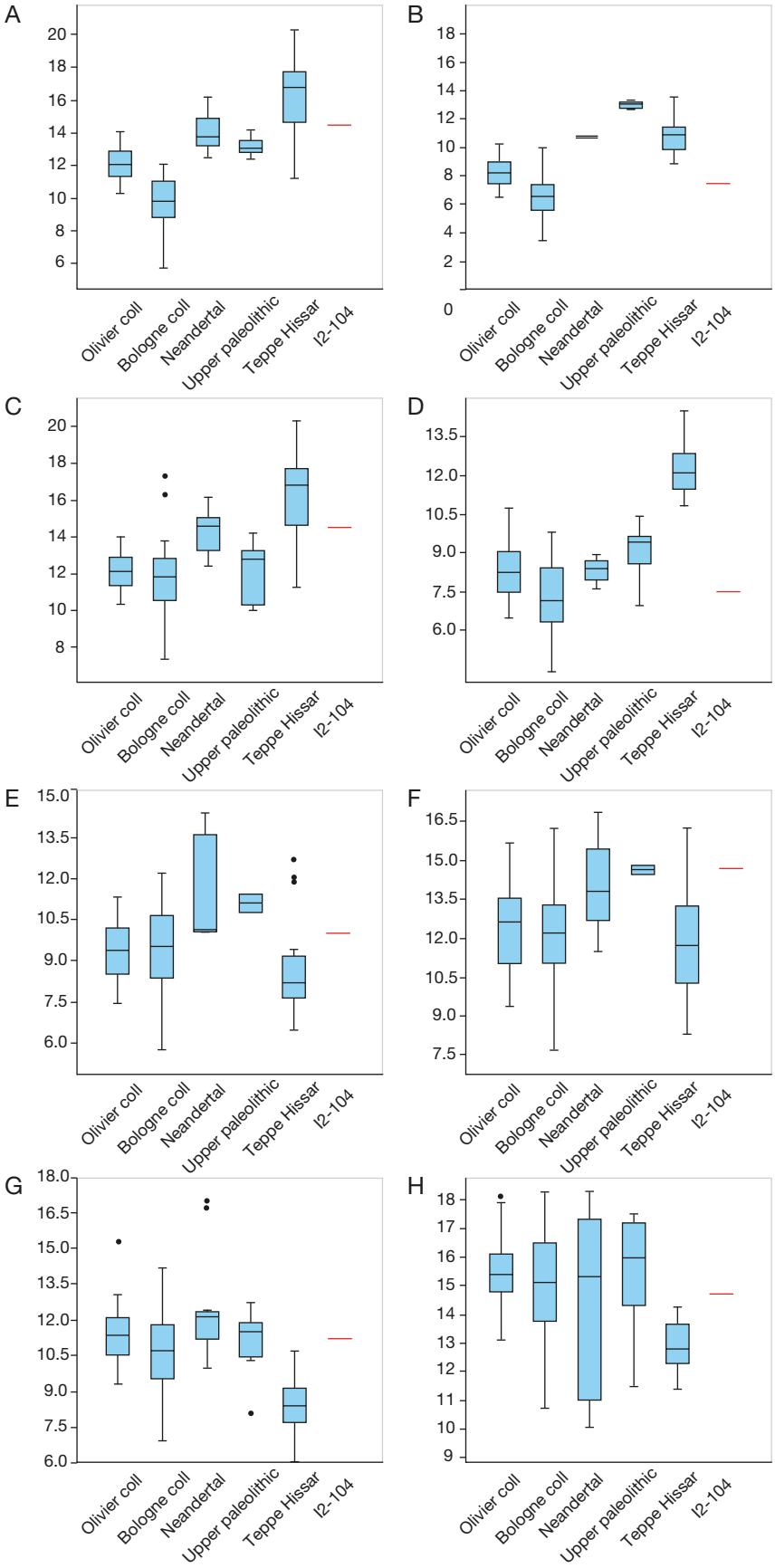

FIG. 6. — Box plot for the 8 epiphysis variables (four for the proximal epiphysis and four for the distal one) describing phalanges (in mm): **A**, distal articular width (P12); **B**, distal articular height (P13); **C**, distal width (P11); **D**, distal height (P10); **E**, proximal articular height (P8); **F**, proximal articular width (P9); **G**, proximal height (P6); **H**, proximal width (P7).

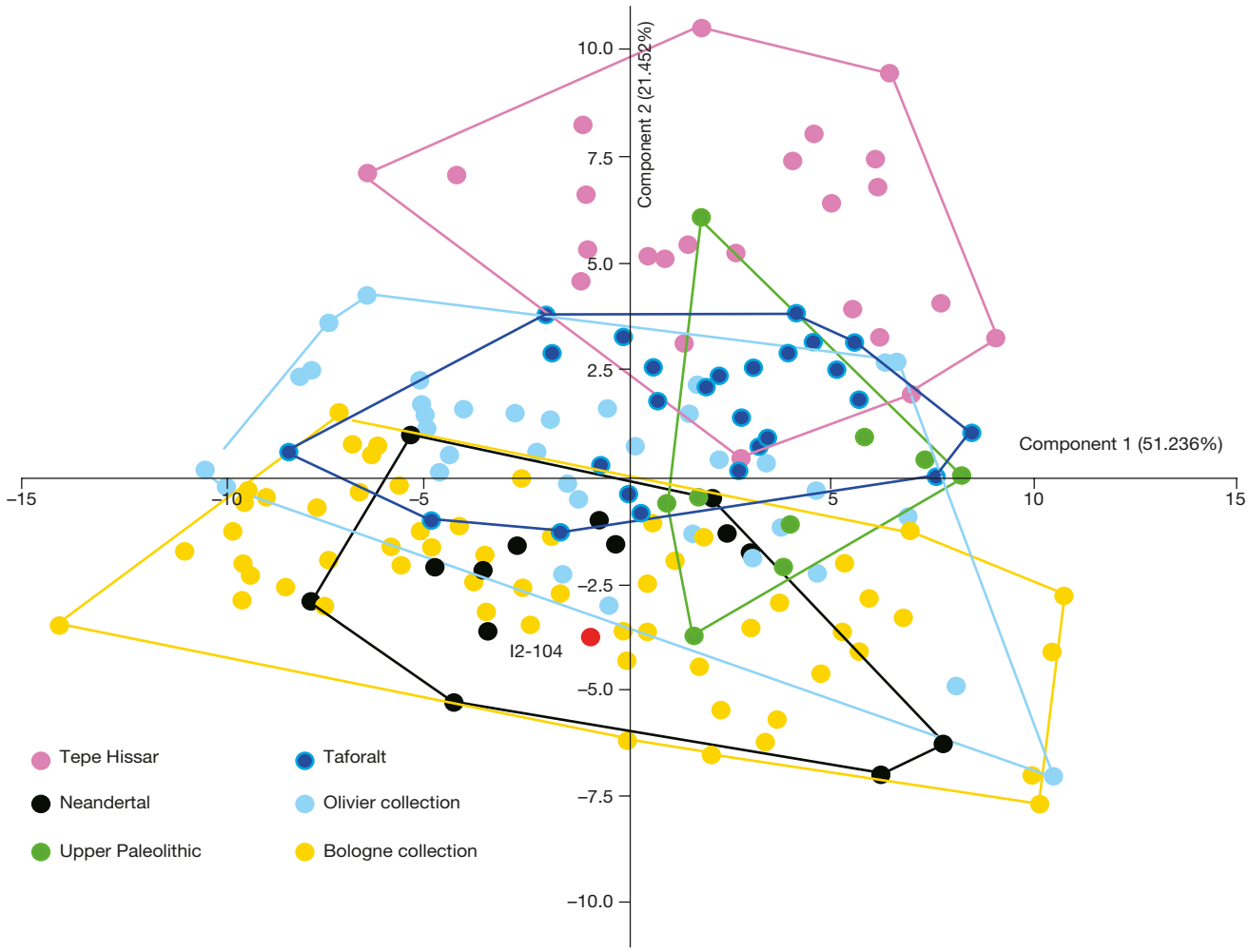

FIG. 7. — The first two components of the principal components analysis (PCA) representing 72.688% of the total variance. The projections on the two other planes (PC1 and PC3 as well as PC2 and PC3) are in the Appendices 18; 19.

In sum, all Neandertal pollical proximal phalanx dimensions fall within the range of modern human variation and fit most closely within the dimensions of the Certosa collection, and the I2-104 pollical proximal phalanx fits well with these two sets.

The distal extremity of the phalanx is clearly distorted and it is difficult to determine how it might have affected measurements. The I2-104 dimensions of the distal end seem not to have been affected too much by the pathology, because all of them are within the Neandertal variations (Fig. 6). However, some PCAs (Appendices 7; 9; 12; 15) show that the I2-104 phalanx falls near the limits or at the limits of the Neandertal variations, but these variations are not only defined by the dimensions of the distal end. All dimensions contribute to the variation of each of the phalanges, not only the distal ones. In other words, the shape of the distal end is modified to an important extent due to this pathology, although the overall dimensions may not have changed so much. This change in morphology is visible in the projection PC1-PC3 and PC2-PC3 (Appendix 18) and places phalanx I2-104 slightly outside the range of Neandertal variability. However, PC3 shows only a small percentage of this variability and thus confirms that morphological changes are small.

DISCUSSION

The morphological and metric analysis of the first thumb phalanx from Moula Guercy does not allow us to attribute it to any specific human groups, i.e., Neandertal or modern human, because the first thumb phalanx does not display any specific morphological or metrical traits. On the contrary, some multivariate analyses exclude the I2-104 phalanx from the Neandertal variability, perhaps due to the deformation of the pathological distal end. The I2-104 first phalanx may be attributed to Neandertal because this specimen comes from layer XV, which has been assigned an age of 120-130 ka (Willmes *et al.* 2016), and all other human remains from this layer have also been attributed to Neandertal (i.e., Defleur *et al.* 1992; Hlusko *et al.* 2013; Mersey *et al.* 2013a, b).

The I2-104 pathology has been interpreted as osteoarthritis due to overuse and aging favored by a genetic background (Condemi *et al.* 2023), but it is difficult to determine which activity may be responsible for this atypical osteoarthritis. In modern humans, osteoarthritis is common at the proximal joint of the first pollical phalanx, not at the

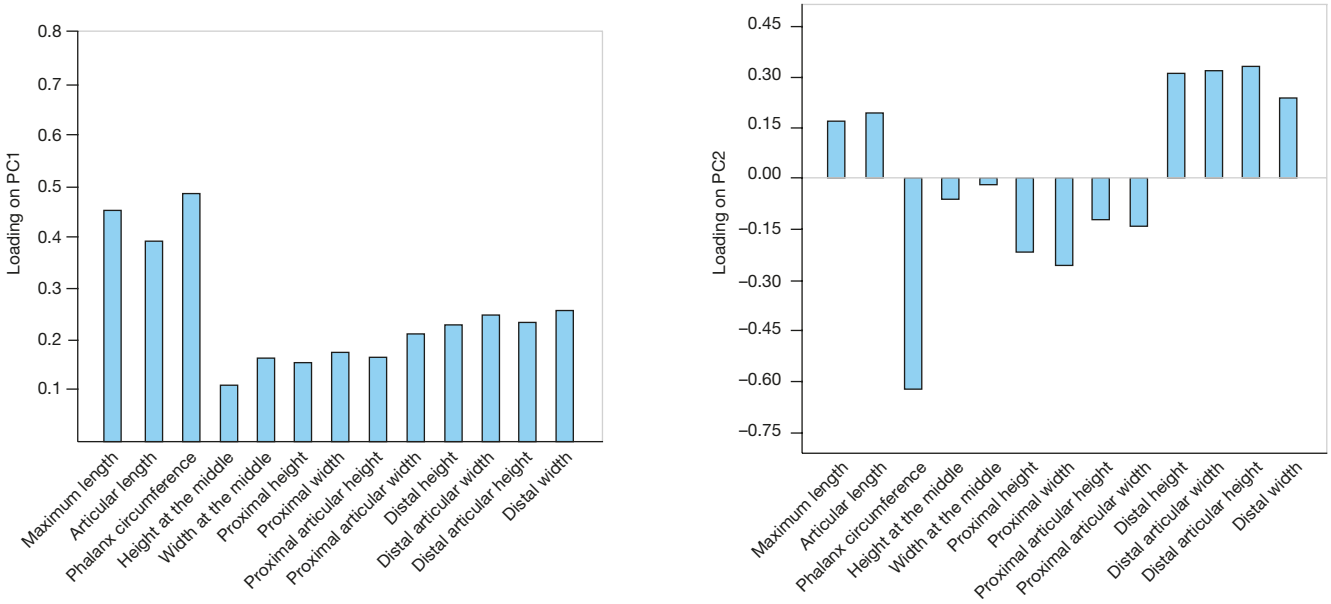

Fig. 8. — The loadings plots of the first two components of the principal components analysis (PCA).

distal one, and is often correlated to obesity (Thijssen *et al.* 2014; Rydberg *et al.* 2020), a cause eliminated by Condemi *et al.* (2023) in this case.

The atypical joint location of the osteoarthritis observed on the I2-104 phalanx could be the effect of Neandertal specific grip skills that led to a particular behavior. Neandertals display a trapeziometacarpal complex (joints between the trapezium and the first metacarpal) that allows a more extended and adducted thumb posture during opposition of the thumb with the other fingers than is the case with modern humans (Bardo *et al.* 2020). In other words, the Neandertal hand is more adapted to powerful transverse squeeze grips (Churchill 2001; Niewoehner 2001, 2006; Bardo *et al.* 2020) like those used to grip hafted tools (Niewoehner 2006; Bardo *et al.* 2020) or wooden tools, which might be numerous according to Anderson-Gerfaud (1990). Direct evidence of hafting tools in the Middle Paleolithic is limited to two artifacts from Umm el Tlel, Syria (Boëda *et al.* 1996), but there is a good deal of indirect evidence for hafting in the Middle Paleolithic (Anderson-Gerfaud & Helmer 1987; Friedman *et al.* 1994-1995; Rots 2011; Degano *et al.* 2019), which clearly shows that hafting was a usual practice for Neandertals.

Neandertal fingers also display entheseal patterns that are in accordance with the use of forceful precision grips based on the thumb and index finger involved for knapping or for other habitual uses like cutting or disarticulating carcasses (Trinkaus & Villemeur 1991; Villemeur 1992; Karakostis *et al.* 2018). This latter powerful precision grip, from our point of view, best accounts for the overuse hypothesis (see below).

Moreover, the question of manual laterality in extinct hominins has long interested archeologists and paleoanthropologists (Cashmore *et al.* 2008 and references therein) because lateralization of hand use is extremely marked in modern human populations and thus can be considered characteristic of our species, although some degree of lateralization exists in non-human primates (Meguerditchian 2014; Verendeev *et al.* 2016). Studies based on striations on frontal teeth devoted to identification of the handedness of Neandertals (i.e., Bermúdez de Castro *et al.* 1988; Estalrich & Rosas 2013; Fiore *et al.* 2015; Condemi *et al.* 2017; Lozano *et al.* 2017), as well as approaches using archeological material (i.e., Semenov 1964; Uomini 2011; Ligkovanlis 2022), have concluded that left-handedness in Neandertals is rare, around 10%, as in modern populations. Furthermore, Guiard's (1987) frame/content model of handedness analyzed the complementarities of the two hands when knapping tools. According to Guiard, one hand, in 90% of the cases the right hand, performs movements that Guiard describes as high frequency because they are spatially and temporally very precise, while the other hand is low frequency, acting as a stabilizer or support.

Table 6. — Eigenvalue and % of variance of each principal component for the principal components analysis (PCA) in Figure 7. 95% bootstrapped confidence intervals are given for the eigenvalues.

PC	Eigenvalue	% variance	Eig 2.5%	Eig 97.5%
1	29.5827	51.236	46.223	56.577
2	12.3861	21.452	17.422	25.812
3	6.1479	10.648	8.526	13.06
4	3.56929	6.1819	5.008	7.6293
5	1.47957	2.5626	1.9373	3.2538
6	1.20481	2.0867	1.3711	2.9119
7	0.864418	1.4971	0.9714	2.1653
8	0.813014	1.4081	0.85816	1.9744
9	0.531695	0.92087	0.66497	1.628
10	0.364008	0.63045	0.37027	0.7684
11	0.334918	0.58006	0.36025	0.71866
12	0.276208	0.47838	0.28756	0.59869
13	0.183449	0.31773	0.21472	0.35205

Studies of shaping lithic tools also show that knappers used almost exclusively one precision grip with the dominant hand during production of early Paleolithic tools (Williams-Hatala 2016). In this case, strikes occurred directly opposite the second and third metacarpal heads, implying that reaction forces would be concentrated in this region rather than at the thumb (Marzke & Shackley 1986). In other words, it is not the thumb of the knapping hand that received most strikes and vibrations during the process of stone shaping.

During knapping, the non-dominant hand holds the nucleus steady, ready to be struck by the rock hammer held in the dominant hand (Williams-Hatala 2016). During knapping, at least for Oldowan and Acheulean tools, the non-dominant hand adopted many different grips in order to maintain the nucleus correctly, as its size and shape changed constantly (Marzke & Shackley 1986; Boëda 1991; Faisal *et al.* 2010; Key & Dunmore 2015). These results demonstrated that motion control and complexity in the non-dominant hand did not seem to differ over geological time during the operating chains. Thus for Mousterian artefacts found in the Moula-Guercy cave, non-dominant hand control was not easier, and thus the thumb of this hand was subject to the same constraints. All these changing grips and their associated moves and vibrations could be the origin of pathologies such as osteoarthrosis. Thus this individual must be right-handed, like 90% of the Neandertal and modern human populations (i.e., Semenov 1964; Uomini 2011; Estalrrich & Rosas 2013; Fiore *et al.* 2015; Condemi *et al.* 2017; Lozano *et al.* 2017).

It is likely that the Neandertal from Moula-Guercy I2-104 was an elderly right-handed individual, which is corroborated by the fact that osteoarthrosis and osteophytes are more frequent and more developed at sites where large and/or repeated forces are applied (Steel 2000). If we only refer to the Guiard model, the pathology present in this pollical phalanx was due to an inflammatory reaction caused by repeated and intense vibrations provoked by the high-frequency knapping, associated with repeated quick moves for changing grips of the left hand, linked to the advanced age of this individual. Moreover, the development of osteoarthritis on this phalanx may have been favored by the genetic background common to Neandertals, which favors the appearance of this pathology (Capellini *et al.* 2017).

Whatever the reason for the development of this pathology, it must have been a very debilitating bone transformation and must have caused significant pain associated with a decrease in grip forces (Jones *et al.* 2001; Zhang *et al.* 2002; Dominick *et al.* 2005; Lee *et al.* 2012), a reduction in joint amplitude (Jones *et al.* 2005), and deformation of the finger, which therefore made it difficult to perform daily life tasks.

Other hand phalanges from Moula-Guercy do not show osteoarthrosis or any other pathologies (Mersey *et al.* 2013b), nor are they shown on other skeletal remains (Mersey *et al.* 2013a, b; Richards *et al.* 2021, 2022). In other words, this pathological phalanx is astonishing in regard to other remains from Moula-Guercy, but as has already been pointed out, only a small part of level XV has been excavated and it is highly possible that other Neandertal remains are still in situ. However, among Neandertals, numerous pathological individuals are known (i.e., Shanidar 1, La Chapelle-aux-Saints, etc.) and thus the phalanx I2-104 fits well with the Neandertal health pattern, especially among old individuals.

CONCLUSION

This analysis reveals that different modern human populations vary in the metric characteristics of the left pollical proximal phalanx. For example, the population of Tepe Hissar differs significantly from the other modern populations studied here. This difference is due mainly to the morphology of the epiphyses and not to the general dimensions of the bone, such as its length or mid-shaft diameter. Neandertal proximal pollical phalanges are not distinguishable from those of modern humans, because their metric dimensions are within the range of variation of modern humans.

Although the pollical proximal phalanx of Neandertals is shorter than that of modern humans, it is their larger epiphyses which play the most important role for distinguishing Neandertal pollical proximal phalanges from other human groups.

The dimensions of the pollical proximal phalanx of Moula-Guercy are not particularly impressive in regard to other Neandertal remains and in regard to other post-cranial remains from Moula-Guercy (Mersey *et al.* 2013a, b).

The phalanx from the Baume de Moula-Guercy (I2-104), although very impressively large on cursory visual inspection, is not significantly different from the other Neandertal phalanges and is situated within the range of Neandertal specimens in all dimensions. The impression of exceptional robustness is due to two factors. The first is the remarkable width of the diaphysis, which gives it a massive appearance (this bone could belong to a large individual studied by Mersey *et al.* (2013a) represented by a large clavicular fragment (M-J1-40)). The second is related to the distal osteophyte associated with the eburnation at the joint surface, which distorts the relationship of the epiphysis to the diaphysis. This particular osteoarthritic joint change of this phalanx, limited but highly developed on the distal end, is more consistent with an age-related overuse of the right hand and would have been very disabling and painful with a loss of power grip (Condemi *et al.* 2023).

In sum, the I2-104 phalanx corresponds broadly to the known Neandertal variation. This phalanx found in layer XV dated to 120-130 ka is also associated with typical Neandertal assemblages and can thus be confidently attributed to Neandertal. This individual was suffering from osteoarthrosis, probably due to overuse through repeated knapping.

Acknowledgements
We want to thank Fanny Derym, curator of the musée archéologique de Soyons, who permitted us to study the I2-104 phalanx. We are also very grateful to Erik Trinkaus for sharing his personal raw data on measurements of first phalanges in *Homo sapiens*. Our thanks also go to Mr M. Friess

(Curator of the anthropological collection of the Musée de l'Homme) and to Pr H. de Lumley (Director of the Institut de Paléontologie Humaine) who permitted us to study respectively the Olivier human collection and the Taforalt remains. We also thank the two reviewers and members of the editorial board for their useful comments. This work was in part supported by the ANR Starch4Sapiens (ANR-20-CE03-0002-01).

Data accessibility

All data collected on I2-104 phalanx are in Table 5 and in Figure 4 and all the raw data are provided as a supplemental Excel data file (Appendix 1).

REFERENCES

ANDERSON-GERFAUD P. 1990. — Aspects of behaviour in the Middle palaeolithic: functional analysis of stone tools from Southwest France, *in* MELLARS P. (ed.), *The Emergence of Modern Humans - An Archaeological Perspective.* Edinburgh University Press, Edinburgh: 389-418. https://doi.org/10.1515/9781474470957-016

ANDERSON-GERFAUD P. & HELMER D. 1987. — L'emmanchement au Moustérien, *in* STORDEUR D. (ed.), La Main et l'outil. Manches et emmanchements préhistoriques. Table ronde CNRS – Lyon 26-29 novembre 1984. *Travaux de la Maison de l'Orient* 15: 37-54.

BARDO A., MONCEL M. H., DUNMORE C. J., KIVELL T. L., POUYDEBAT E. & CORNETTE R. 2020. — The implications of thumb movements for Neanderthal and modern human manipulation. *Scientific Reports* 10: 19323 (12 p.). https://doi.org/10.1038/s41598-020-75694-2

BARSHAY-SZMIDT C., COSTAMAGNO S., HENRY-GAMBIER D., LAROULANDIE V., PÉTILLON J.-M., BOUDADI-MALIGNE M., KUNTZ D., LANGLAIS M. & MALLYE J. B. 2016. — New extensive focused AMS 14C dating of the Middle and Upper Magdalenian of the western Aquitaine/Pyrenean region of France (ca. 19–14 ka cal BP): proposing a new model for its chronological phases and for the timing of occupation. *Quaternary International* 414: 62-91. https://doi.org/10.1016/j.quaint.2015.12.073

BELCASTRO M. G., BONFIGLIOLI B., PEDROSI M. E., ZUPPELLO M., TANGANELLI V. & MARIOTTI V. 2017. — The history and composition of the identified human skeletal collection of the Certosa cemetery (Bologna, Italy, 19th–20th century). *International Journal of Osteoarchaeology* 27 (5): 912-925. https://doi.org/10.1002/oa.2605

BERMÚDEZ DE CASTRO J. M., BROMAGE T. G. & FERNÁNDEZ-JALVO Y. 1988. — Buccal striations on fossil human anterior teeth: evidence of handedness in the Middle and early Upper Pleistocene. *Journal of Human Evolution* 17 (4): 403-412. https://doi.org/10.1016/0047-2484(88)90029-2

BOËDA E. 1991. — Taille de silex par Eric Boeda : épreuves de tournage. Archives Départementales du Val de Marne. Available at: https://archives.valdemarne.fr/ (cote 3AV 34, access June 16, 2023).

BOËDA E., CONNAN J., DESSORT D., MUHESEN S., MERCIER N., VALLADAS H. & TISNÉRAT N. 1996. — Bitumen as a hafting material on Middle Palaeolithic artefacts. *Nature* 380 (6572): 336-338. https://doi.org/10.1038/380336a0

BOUZOUGGAR A., BARTON R. N. E., BLOCKLEY S., BRONK-RAMSEY C., COLLCUTT S. N., GALE R., HIGHAM T. F. G., HUMPHREY L. T., PARFITT S., TURNER E. & WARD S. 2008. — Reevaluating the age of the Iberomaurusian in Morocco. *African Archaeological Review* 25 (1-2): 3-19. https://doi.org/10.1007/s10437-008-9023-3

CAPELLINI T., CHEN H., CAO J., DOXEY A. C., KIAPOUR A. M., SCHOOR M. & KINGSLEY D. 2017. — Ancient selection for derived alleles at a GDF5 enhancer influencing human growth and osteoarthritis risk. *Nature Genetics* 49: 1202-1210. https://doi.org/10.1038/ng.3911

CASHMORE L., UOMINI N. & CHAPELAIN A. 2008. — The evolution of handedness in humans and great apes: a review and current issues. *Journal of Anthropological Sciences* 86: 7-35.

CHURCHILL S. E. 2001. — Hand morphology, manipulation, and tool use in Neandertals and early modern humans of the Near East. *Proceedings of the National Academy of Sciences (USA)* 98 (6): 2953-2955. https://doi.org/10.1073/pnas.061032198

CONDEMI S., MONGE J., QUERTELET S., FRAYER D. W. & COMBIER J. 2017. — Vergisson 4: a left-handed Neandertal. *American Journal of Physical Anthropology* 162 (1): 186-190. https://doi.org/10.1002/ajpa.23101

CONDEMI S., PANUEL M., CHAUMOITRE K., BELCASTRO M. G., PIETROBELLI A. & VOISIN J.-L. 2023. — A pathological Neandertal thumb phalanx from Moula-Guercy (France). *International Journal of Paleopathology* 42: 14-17. https://doi.org/10.1016/j.ijpp.2023.06.002

COWGILL L. W., TRINKAUS E. & ZEDER M. A. 2007. — Shanidar 10: a Middle Paleolithic immature distal lower limb from Shanidar Cave, Iraqi Kurdistan. *Journal of Human Evolution* 53 (2): 213-223. https://doi.org/10.1016/j.jhevol.2007.04.003

CRÉGUT-BONNOURE E., BOULBES N., DAUJEARD C., FERNANDEZ P. & VALENSI P. 2010. — Nouvelles données sur la grande faune de l'Éemien dans le Sud-Est de la France. *Quaternaire* 21 (3): 227-248. https://doi.org/10.4000/quaternaire.5592

CREVECOEUR I. 2014. — Hand bones. *Anthropologica et Praehistorica* 124: 1-20.

CREVECOEUR I. & VILLOTTE S. 2006. — Atteintes pathologiques de Nazlet Khater 2 et activité minière au début du Paléolithique supérieur en Égypte. *Bulletins et Mémoires de la Société d'Anthropologie de Paris* 18 (3-4): 165-175. https://doi.org/10.4000/bmsap.1612

DE LUMLEY M. A. 1973. — *Anténéandertaliens et néandertaliens du bassin méditerranéen occidental européen*. Éditions du Laboratoire de Paléontologie Humaine et de Préhistoire (Études quaternaires ; mémoire no. 2), Marseille, 603 p.

DEFLEUR A. 1995. — Nouvelles découvertes de restes humains Moustériens dans les dépôts de la Baume Moula-Guercy (Soyons, Ardèche). *Bulletins et Mémoires de la Société d'Anthropologie de Paris* 7 (3-4): 185-190. https://doi.org/10.3406/bmsap.1995.2419

DEFLEUR A. 2015. — Les industries lithiques moustériennes de la Baume Moula-Guercy (Soyons, Ardèche). Fouilles 1993-1999. *L'Anthropologie* 119 (2): 170-253. https://doi.org/10.1016/j.anthro.2015.04.002

DEFLEUR A. & DESCLAUX E. 1997. — Étude préliminaire des micromammifères de la Baume Moula-Guercy à Soyons (Ardèche, France). Systématique, biostratigraphie et paléoécologie. *Quaternaire* 8 (2-3): 213-223. https://doi.org/10.3406/quate.1997.1574

DEFLEUR A. & DESCLAUX E. 2019. — Impact of the last interglacial climate change on ecosystems and Neanderthals behavior at Baume Moula-Guercy, Ardèche, France. *Journal of Archaeological Science* 104: 114-124. https://doi.org/10.1016/j.jas.2019.01.002

DEFLEUR A., DUTOUR O. & VANDERMEERSCH B. 1992. — Étude de deux dents humaines provenant des niveaux moustériens de la Baume Néron (Soyons, Ardèche). *Bulletins et Mémoires de la Société d'Anthropologie de Paris* 4 (1-2): 127-134. https://doi.org/10.3406/bmsap.1992.2308

DEFLEUR A., DUTOUR O., VALLADAS H. & VANDERMEERSCH B. 1993. — Cannibals among the Neanderthals? *Nature* 362 (6417): 214. https://doi.org/10.1038/362214a0

DEFLEUR A., CRÉGUT-BONNOURE É. & DESCLAUX E. 1998. — Première mise en évidence d'une séquence éémienne à restes humains dans le remplissage de la Baume Moula-Guercy (Soyons, Ardèche). *Comptes Rendus de l'Académie des Sciences, Serie 2, Earth Planet Science* 326 (6): 453-458.

Defleur A., White T. D., Valensi P., Slimak L. & Crégut-Bonnoure E. 1999. — Neanderthal cannibalism at Moula-Guercy, Ardèche, France. *Science* 286 (5437): 128-131. https://doi.org/10.1126/science.286.5437.128

Defleur A., Crégut-Bonnoure É., Desclaux E. & Thinon M. 2001. — Présentation paléo-environnementale du remplissage de la Baume Moula-Guercy à Soyons (Ardèche) : implications paléoclimatiques et chronologiques. *L'Anthropologie (Paris)* 105 (3): 369-408. https://doi.org/10.1016/S0003-5521(01)80022-4

Defleur A., Desclaux E., Jabbour R. S. & Richards G. D. 2020. — The Eemian: Global warming, ecosystem upheaval, demographic collapse and cannibalism at Moula-Guercy. A reply to Slimak and Nicholson (2020). *Journal of Archaeological Science* 117: 105113 (9 p.). https://doi.org/10.1016/j.jas.2020.105113

Degano I., Soriano S., Villa P., Pollarolo L., Lucejko J. J., Jacobs Z., Douka K., Vitagliano S. & Tozzi C. 2019. — Hafting of Middle Paleolithic tools in Latium (central Italy): new data from Fossellone and Sant'Agostino caves. *PLoS ONE* 14 (6): e0213473 (29 p.). https://doi.org/10.1371/journal.pone.0213473

Diogo R., Richmond B. G. & Wood B. 2012. — Evolution and homologies of primate and modern human hand and forearm muscles, with notes on thumb movements and tool use. *Journal of Human Evolution* 63 (1): 64-78. https://doi.org/10.1016/j.jhevol.2012.04.001

Djindjian F., Koslowski J. & Otte M. 1999. — *Le Paléolithique supérieur en Europe*. Armand Colin, Paris, 474 p.

Dominick K. L., Jordan J. M., Renner J. B. & Kraus V. B. 2005. — Relationship of radiographic and clinical variables to pinch and grip strength among individuals with osteoarthritis. *Arthritis & Rheumatism* 52 (5): 1424-1430. https://doi.org/10.1002/art.21035

Estalrrich A. & Rosas A. 2013. — Handedness in Neandertals from the El Sidrón (Asturias, Spain): evidence from Instrumental Striations with Ontogenetic Inferences. *PLoS ONE* 8 (5): e62797. https://doi.org/10.1371/journal.pone.0062797

Facchini F., Mariotti V., Bonfiglioli B. & Belcastro M. G. 2006. — Les collections ostéologiques et ostéoarchéologiques du musée d'Anthropologie de l'université de Bologne (Italie). *Bulletin Archéologique de Provence* Supplement 4: 67-70.

Faisal A., Stout D., Apel J. & Bradley B. 2010. — The manipulative complexity of Lower Paleolithic stone toolmaking. *PLoS ONE* 5: 1-11. https://doi.org/10.1371/journal.pone.0013718

Ferembach D. 1960. — Les Hommes du mésolithiques d'Afrique du Nord et le problème des isolats. *Boletim da Sociedade Portuguesa de Ciências Naturais* 8 (2): 1-16.

Ferembach D. 1963. — Frequency of spina bifida occulta in prehistoric human skeletons. *Nature* 199 (4888): 100-101. https://doi.org/10.1038/199100a0

Ferembach D., Dastugue J. & Poitrat-Targowla M.-J. 1962. — *La Nécropole épipaléolithique de Taforalt (Maroc oriental)*. Edita-Casablanca, Casablanca, 175 p.

Fiore I., Bondioli L., Radovčić J. & Frayer D. W. 2015. — Handedness in the Krapina Neandertals: a re-evaluation. *Paleo-Anthropology* 2015: 19-36. https://doi.org/10.4207/PA.2015.ART93

Fragaszy D. M. & Crast J. 2016. — Functions of the hand in primates, *in* Kivell T. L., Lemelin P., Richmond B. G. & Schmitt D. (eds), *The Evolution of the Primate Hand. Developments in Primatology: Progress and Prospects.* Springer, New York: 313-344. https://doi.org/10.1007/978-1-4939-3646-5_12

Friedman E., Goren-Inbar N., Rosenfeld A., Marder O. & Burian F. 1994-1995. — Hafting during mousterian times - further indication. *Journal of the Israel Prehistoric Society* 26: 8-31.

Gambier D., Valladas H., Tisnérat-Laborde N., Arnold M. & Bresson F. 2000. — Datation de vestiges humains présumés du Paléolithique supérieur par la méthode du Carbone 14 en spectrométrie de masse par accélérateur. *Paléo* 12: 201-212. https://doi.org/10.3406/pal.2000.1602

Grün R. & Stringer C. 2000. — Tabun revisited: revised ESR chronology and new ESR and U-series analyses of dental material from Tabun C1. *Journal of Human Evolution* 39 (6): 601-612. https://doi.org/10.1006/jhev.2000.0443

Grün R., Stringer C., McDermott F., Nathan R., Porat N., Robertson S. Taylor L., Mortimer G., Eggins S. & McCulloch M. 2005. — U-series and ESR analyses of bones and teeth relating to the human burials from Skhul. *Journal of Human Evolution* 49 (3): 316-334. https://doi.org/10.1016/j.jhevol.2005.04.006

Guérin G., Frouin M., Talamo S., Aldeias V., Bruxelles L., Chiotti L., Dibble H. L., Goldberg P., Hublin J.-J., Jain M. Lahaye C., Madelaine S., Maureille B., McPherron S. J. P., Mercier N., Murray A. S., Sandgathe D., Steele T. E., Thomsen K. J. & Turq A. 2015. — A multi-method luminescence dating of the Palaeolithic sequence of La Ferrassie based on new excavations adjacent to the La Ferrassie 1 and 2 skeletons. *Journal of Archaeological Science* 58: 147-166. https://doi.org/10.1016/j.jas.2015.01.019

Guiard Y. 1987. — Asymmetric division of labor in human skilled bimanual action: the kinematic chain as a model. *Journal of motor behavior* 19 (4): 486-517. https://doi.org/10.1080/00222895.1987.10735426

Gürsan-Salzmann A. 2016. — *The New Chronology of the Bronze Age Settlement of Tepe Hissar, Iran*. University of Pennsylvania Museum of Archaeology and Anthropology, Philadelphia, 387 p.

Hammer Ø. & Harper D. 2006. — *Paleontological Data Analysis*. Blackwell Publishing, Malden, 351 p. https://doi.org/10.1002/9780470750711

Hammer Ø. & Harper D. 2023. — PAleontological STatistics Version 4.14, Reference manual. Available at: https://www.nhm.uio.no/english/research/resources/past/downloads/past-4manual.pdf

Hammer Ø., Harper D. & Ryan P. D. 2001. — PAST: Paleontological statistics software package for education and data analysis. *Palaeontologia Electronica* 4 (1): article no. 4, 9 p.

Harvati K., Röding C., Bosman A. M., Karakostis F. A., Grün R., Stringer C., Karkanas P., Thompson N. C., Koutoulidis V., Moulopoulos L. A., Gorgoulis V. G., Kouloukoussa M. 2019. — Apidima Cave fossils provide earliest evidence of *Homo sapiens in Eurasia*. *Nature* 571 (7766): 500-504. https://doi.org/10.1038/s41586-019-1376-z

Heim J.-L. 1983. — Les variations du squelette post-crânien des hommes de Néandertal suivant le sexe. *L'Anthropologie* 87 (1): 5-26.

Henry-Gambier D. 2002. — Les fossiles de Cro-Magnon (les Eyzies-de-Tayac, Dordogne) : nouvelles données sur leur position chronologique et leur attribution culturelle. *Bulletins et Mémoires de la Société d'Anthropologie de Paris* 14 (1-2): 89-112. https://doi.org/10.4000/bmsap.459

Higham T., Jacobi R., Basell L., Ramsey C. B., Chiotti L. & Nespoulet R. 2011. — Precision dating of the Palaeolithic: A new radiocarbon chronology for the Abri Pataud (France), a key Aurignacian sequence. *Journal of Human Evolution* 61 (5): 549-563. https://doi.org/10.1016/j.jhevol.2011.06.005

Higham T., Douka K., Wood R., Ramsey C. B., Brock F., Basell L., Camps M., Arrizabalaga A., Baena J., Barroso-Ruíz C., Bergman C., Boitard C., Boscato P., Caparrós M., Conard N. J., Draily C., Froment A., Galván B., Gambassini P., Garcia-Moreno A., Grimaldi S., Haesaerts P., Holt B., Iriarte-Chiapusso M.-J., Jelinek A., Jordá Pardo J. F., Maíllo-Fernández J. M., Marom A., Maroto J., Menéndez M., Metz L., Morin E., Moroni A., Negrino F., Panagopoulou E., Peresani M., Pirson S., de la Rasilla M., Riel-Salvatore J., Ronchitelli A., Santamaria D., Semal P., Slimak L., Soler J., Soler N., Villaluenga A., Pinhasi R. & Jacobi R. 2014. — The timing and spatiotemporal patterning of Neanderthal disappearance. *Nature* 512 (7514): 306-309. https://doi.org/10.1038/nature13621

Hlusko L. J., Carlson J. P., Guatelli-Steinberg D., Krueger K. L., Mersey B., Ungar P. S. & Defleur A. 2013. — Neanderthal teeth from Moula-Guercy, Ardèche, France. *American Journal of Physical Anthropology* 151 (3): 477-491. https://doi.org/10.1002/ajpa.22291

Janković I., Ahern J. C. M., Karavanić I., Stockton T. & Smith F. H. 2012. — Epigravettian human remains and artifacts from Šandalja II, Istria, Croatia. *PaleoAnthropology* 2012: 87-122. https://doi.org/10.4207/PA.2012.ART72

Jones G., Cooley H. M. & Bellamy N. 2001. — A cross-sectional study of the association between Heberden's nodes, radiographic osteoarthritis of the hands, grip strength, disability and pain. *Osteoarthritis & Cartilage* 9 (7): 606-611. https://doi.org/10.1053/joca.2001.0460

Jones P., Alexander C. J., Stewart J. & Lynskey N. 2005. — Idiopathic osteoarthritis and contracture: causal implications. *Annals of the Rheumatic Diseases* 64 (2): 226-228. https://doi.org/10.1136/ard.2003.016444

Karakostis F. A., Lorenzo C. & Moraitis K. 2017. — Morphometric variation and ray allocation of human proximal hand phalanges. *Anthropologischer Anzeiger* 74 (4): 269-281. https://doi.org/10.1127/anthranz/2017/0715

Karakostis F. A., Hotz G., Tourloukis V. & Harvati K. 2018. — Evidence for precision grasping in Neandertal daily activities. *Science Advances* 4 (9): eaat2369 (12 p.). https://doi.org/10.1126/sciadv.aat2369

Kéfi R., Stevanovitch A., Bouzaid E. & Béraud-Colomb E. 2005. — Diversité mitochondriale de la population de Taforalt (12 000 BP – Maroc) : une approche génétique à l'étude du peuplement de l'Afrique du Nord. *Anthropologie* 43 (1): 1-11. https://www.jstor.org/stable/26292709

Key A. J. M. & Dunmore C. J. 2015. — The evolution of the hominin thumb and the influence exerted by the non-dominant hand during stone tool production. *Journal of Human Evolution* 78: 60-69. https://doi.org/10.1016/j.jhevol.2014.08.006

Langley N. R., Jantz L. M., McNulty S., Maijanen H., Ousley S. D. & Jantz R. L. 2018. — Data for validation of osteometric methods in forensic anthropology. *Data in Brief* 19: 21-28. https://doi.org/10.1016/j.dib.2018.04.148

Lee H. J., Paik N.-J., Lim J.-Y., Kim K. W. & Gong H. S. 2012. — The impact of digit-related radiographic osteoarthritis of the hand on grip-strength and upper extremity disability. *Clinical Orthopaedics and Related Research* 470 (8): 2202-2208. https://doi.org/10.1007/s11999-012-2253-3

Lemelin P. & Diogo R. 2016. — Anatomy, function and evolution of the primate hand musculature, *in* Kivell T. L., Lemelin P., Richmond B. G. & Schmitt D. (eds), *The Evolution of the Primate Hand Anatomical, Developmental, Functional, and Paleontological Evidence*. Springer New York (Primatology: Progress and Prospects series): 155-193. https://doi.org/10.1007/978-1-4939-3646-5_7

Ligkovanlis S. 2022. — Hand-preference and lithic production-exploring neanderthal handedness rates through the study of hertzian fracture features on lithic blanks. *Open Quaternary* 8 (1): 4 (21 p.). https://doi.org/10.5334/oq.111

Lorenzo C., Arsuaga J. L. & Carretero J. M. 1999. — Hand and foot remains from the Gran Dolina early Pleistocene site (Sierra de Atapuerca, Spain). *Journal of Human Evolution* 37 (3-4): 501-522. https://doi.org/10.1006/jhev.1999.0341

Lozano M., Estalrrich A., Bondioli L., Fiore I., Bermúdez de Castro J. M., Arsuaga J. L., Carbonell E., Rosas A. & Frayer D. 2017. — Right-handed fossil humans. *Evolutionary Anthropology* 26 (6): 313-324. https://doi.org/10.1002/evan.21554

Marzke M. W. & Shackley M. S. 1986. — Hominid hand use in the Pliocene and Pleistocene: evidence from experimental archaeology and comparative morphology. *Journal of Human Evolution* 15 (6): 439-460. https://doi.org/10.1016/S0047-2484(86)80027-6

Meguerditchian A. 2014. — Pour une large approche comparative entre primates dans les recherches sur les origines de l'Homme : l'exemple de la latéralité manuelle. *Bulletins et Mémoires de la Société d'Anthropologie de Paris* 26 (3-4): 166-171. https://doi.org/10.1007/s13219-014-0114-1

Mercier N. & Valladas H. 2003. — Reassessment of TL age estimates of burnt flints from the Paleolithic site of Tabun Cave, Israel. *Journal of Human Evolution* 45 (5): 401-409. https://doi.org/10.1016/j.jhevol.2003.09.004

Mercier N., Valladas H., Bar-Yosef O., Vandermeersch B., Stringer C. & Joron J.-L. 1993. — Thermoluminescence date for the Mousterian burial site of Es-Skhul, Mt.Carmel. *Journal of Archaeological Science* 20: 169-174. https://doi.org/10.1006/jasc.1993.1012

Mersey B., Brudvik K., Black M. T. & Defleur A. R. 2013a. — Neanderthal axial and appendicular remains from Moula-Guercy, Ardèche, France. *American Journal of Physical Anthropology* 152 (4): 530-542. https://doi.org/10.1002/ajpa.22388

Mersey B., Jabbour R. S., Brudvik K. & Defleur A. R. 2013b. — Neanderthal hand and foot remains from Moula-Guercy, Ardèche, France. *American Journal of Physical Anthropology* 152 (4): 516-529. https://doi.org/10.1002/ajpa.22389

Musgrave J. H. 1971. — How dextrous was Neanderthal man? *Nature* 233 (5321): 538-541. https://doi.org/10.1038/233538a0

Musgrave J. H. 1973. — The phalanges of Neandertal and Upper Palaeolithic hands, *in* Day M. H. (ed.), *Symposia of the Society for the Study of Human Evolution - Volume XI - Human Evolution,* Taylor & Francis, New York: 59-85.

Niewoehner W. A. 2001. — Behavioral inferences from the Skhuly/Qafzeh early modern human hand remains. *Proceedings of the National Academy of Sciences of the United States of America* 98 (6): 2979-2984. https://doi.org/10.1073/pnas.041588898

Niewoehner W. A. 2006. — Neanderthal hands in their proper perspective, *in* Harvati K. & Harrisson T. (eds), *Neanderthals Revisited: New Approaches and Perspectives. Vertebrate Paleobiology and Paleoanthropology*. Springer, Dordrecht: 157-190. https://doi.org/10.1007/978-1-4020-5121-0_9

Niewoehner W. A., Weaver A. H. & Trinkaus E. 1997. — Neandertal capitate-metacarpal articular morphology. *American Journal of Physical Anthropology* 103 (2): 219-233. https://doi.org/10.1002/(SICI)1096-8644(199706)103:2<219::AID-AJPA7>3.0.CO;2-O

Niewoehner W. A., Bergstrom A., Eichele D., Zuroff M. & Clark J. T. 2003. — Manual dexterity in Neanderthals. *Nature* 422 (6930): 395. https://doi.org/10.1038/422395a

Orban R. & Leguebe A. 1990. — A biometrical comparison of a Neandertal metacarpal from Spy with other handbone material. *Human Evolution* 5 (5): 493-501. https://doi.org/10.1007/BF02435598

Perini T. A., Lameira de Oliveira G., Ornellas J. S. & Palha de Oliveira F. 2005. — Technical error of measurement in anthropometry. *Revista Brasileira de Medicina do Esporte* 11 (1): 86-90. https://doi.org/10.1590/S1517-86922005000100009

Radovčić J., Smith F. H. Trinkaus E. & Wolpoff M. 1988. — *The Krapina Hominids an Illustrated Catalog of Skeletal Collection*. Mladost publishing house and Croatian Natural History Museum, Zagreb, 118 p.

Richards G. D., Guipert G. Jabbour R. S. & Defleur A. R. 2021. — Neanderthal cranial remains from Baume Moula-Guercy (Soyons, Ardèche, France). *American Journal of Physical Anthropology* 175 (1): 201-226. https://doi.org/10.1002/ajpa.24256

Richards G. D., Jabbour R. S., Guipert G. & Defleur A. R. 2022. — Neanderthal child's occipital from Baume Moula-Guercy (Soyons, Ardèche, France). *American Journal of Biological Anthropology* 178 (1): 69-88. https://doi.org/10.1002/ajpa.24489

Richmond B. G., Roach N. T., Ostrofsky K. R. 2016. — Evolution of the early hominin hand, *in* Kivell T. L., Lemelin P., Richmond B. G. & Schmitt D. (eds), *The Evolution of the Primate Hand Anatomical, Developmental, Functional, and Paleontological Evidence*. Springer (Primatology: Progress and Prospects Series), New York: 515-543. https://doi.org/10.1007/978-1-4939-3646-5_18

Rink W. J., Schwarcz H. P., Smith F. H. & Radovčić J. 1995. — ESR ages for Krapina hominids. *Nature* 378 (6552): 24. https://doi.org/10.1038/378024a0

Roche J. 1959. — Nouvelle datation de l'épipaléolithique marocain par la méthode du carbone 14. *Comptes Rendus Hebdomadaires des Séances de l'Académie des Sciences* 249: 729-730.

Roche J. 1976. — Cadre chronologique de l'Épipaléolithique marocain, *in* Camps G. (ed.), *IX^e congrès UISPP – Colloque II : Chronologie et synchronisme dans la préhistoire circumméditerranéenne, Nice*: 153-167.

Rots V. 2011. — Tool use and hafting in the western European Middle Palaeolithic, *in* Toussaint M., Di Modica K. & Pirson S. (eds), Le Paléolithique moyen en Belgique – Mélanges Marguerite Ulrix-Closset. *ERAUL* 128: 277-287.

Rydberg M., Dahlin L. B., Gottsatar A., Nilsson P. M., Melander O. & Zimmerman M. 2020. — High body mass index is associated with increased risk for osteoarthritis of the first carpometacarpal joint during more than 30 years of follow-up. *RMD Open* 6: e001368. https://doi.org/10.1136/rmdopen-2020-001368

Saos T., Djerrab A. & Defleur A. 2014. — Étude stratigraphique, sédimentologique et magnétique des dépôts pléistocène moyen et supérieur de la Baume Moula-Guercy (Soyons, Ardèche). *Quaternaire* 25 (3): 237-251. https://doi.org/10.4000/quaternaire.7065

Schmitz R. W., Serre D., Bonanin G., Feine S., Hillgruber F., Krainitzki H., Pääbo S. & Smith F. H. 2002. — The Neandertal type site revisited: interdisciplinary investigations of skeletal remains from the Neander Valley, Germany. *Proceedings of the National Academy of Sciences of the United States of America* 99 (20): 13342-13347. https://doi.org/10.1073/pnas.192464099

Semal P., Rougier H., Crevecoeur I., Jungels C., Flas D., Hauzeur A., Maureille B., Germonpré M., Bocherens H., Pirson S., Cammaert L., de Clerck N., Hambücken A., Higham T., Toussaint M. & van der Plicht J. 2009. — New data on the late Neandertals: direct dating of the Belgian Spy fossils. *American Journal of Physical Anthropology* 138 (4): 421-428. https://doi.org/10.1002/ajpa.20954

Semenov S. A. 1964. — *Prehistoric Technology*. Cory Adams & MacKay, London, 211 p.

Slimak L. & Nicholson C. 2020. — Cannibals in the forest: a comment on Defleur and Desclaux (2019). *Journal of Archaeological Science* 117: 105034 (9 p.). https://doi.org/10.1016/j.jas.2019.105034

Slimak L., Zanolli C., Higham T., Frouin M., Schwenninger J.-L., Arnold L. J., Demuro M., Douka K., Mercier N., Guérin G., Valladas H., Yvorra P., Giraud Y., Seguin-Orlando A., Orlando L., Lewis J. E., Muth X., Camus H., Vandevelde S., Buckley M., Mallol C., Stringer C. & Metz L. 2022. — Modern human incursion into Neanderthal territories 54,000 years ago at Mandrin, France. *Science Advances* 8 (6): eabj9496. https://doi.org/10.1126/sciadv.abj9496

Steel J. 2000. — Skeletal indicators of handedness, *in* Cox M. & Simon M. (eds), *Human Osteology: In Archaeology and Forensic Science.* Cambridge University Press, Cambrige: 307-323.

Svoboda J. 2006a. — The archeological contexts of the human remains, *in* Trinkaus E. & Svoboda J. (eds), *Early Modern Human Evolution in Central Europe – The People of Dolní Vestonice and Pavlov.* Oxford University Press, Oxford: 9-14.

Svoboda J. 2006b. — The archeological framework, *in* Trinkaus E. & Svoboda J. (eds), *Early Modern Human Evolution in Central Europe – The People of Dolní Vestonice and Pavlov.* Oxford University Press, Oxford: 6-8.

Tabachnick B. G. & Fidell L. S. 2013. — *Using Multivariate Statistics*. 6th edition. Boston, Mass: Pearson Education.

Thijssen E., van Caam A. & van der Kraan P. M. 2014. — Obesity and osteoarthritis, more than just wear and tear: pivotal roles for inflamed adipose tissue and dyslipidaemia in obesity-induced osteoarthritis. *Rheumatology* 54 (4): 588-600. https://doi.org/10.1093/rheumatology/keu464

Trinkaus E. 1983. — *The Shanidar Neandertals*. Academic Press, New York, 502 p.

Trinkaus E. 2016. — *The Krapina Human Postcranial Remains: Morphology, Morphometrics and Paleopathology*. FF-Press, Zagreb, 152 p.

Trinkaus E. & Villemeur I. 1991. — Mechanical advantages of the Neandertal thumb in flexion: a test of an hypothesis. *American Journal of Physical Anthropology* 84 (3): 249-260. https://doi.org/10.1002/ajpa.1330840303

Trinkaus E., Churchill S. E., Villemeur I., Riley K. G., Heller J. A. & Ruff C. B. 1991. — Robusticity verus shape: the functional interpretation of Neandertal appendicular morphology. *Journal of the Anthropological Society of Nippon* 99 (3): 257-278. https://doi.org/10.1537/ase1911.99.257

Trinkaus E., Buzhilova A. P., Mednikova M. B. & Dobrovolskaya M. V. 2014a. — *The People of SunghirBurials, Bodies and Behavior in the Earlier Upper Paleolithic*. Oxford University Press, Oxford, 359 p. https://doi.org/10.1093/oso/9780199381050.001.0001

Trinkaus E., Haduch E., Valde-Nowak P. W. & Wojtal P. 2014b. — The Obłazowa 1 early modern human pollical phalanx and Late Pleistocene distal thumb proportions. *Homo* 65 (1): 1-12. https://doi.org/10.1016/j.jchb.2013.09.002

Tuttle R. H. 1969. — Quantitative and functional studies on the hands of the Anthropoidea: I. The Hominoidea. *Journal of Morphology* 128 (3): 309-363. https://doi.org/10.1002/jmor.1051280304

Uomini N. T. 2011. — Handedness in Neanderthals, *in* Conard N. J. & Richter J. (eds), *Neanderthal Lifeways, Subsistence And Technology: One Hundred Fifty Years Of Neanderthal Study*. Springer (Vertebrates Paleobiology and Paleoanthropology Series), Dordrecht: 139-154. https://doi.org/10.1007/978-94-007-0415-2_14

Vandermeersch B. 1991. — La ceinture scapulaire et les membres supérieurs, *in* Bar-Yosef O. & Vandermeersch B. (eds), *Le squelette Moustérien de Kebara 2*. Édition du CNRS, Paris: 157-178.

Valladas H. & Valladas G. 1991. — Datation par la thermoluminescence de silex chauffés des grottes de Kébara et de Qafzeh, *in* Bar Yosef O. & Vandermeersch B. (eds), *Le Squelette Moustérien De Kébara 2*. CNRS Édition (Cahiers de Paléoanthropologie), Paris: 43-47.

Valladas H., de Lumley H. & Kaltnecker E. 2016. — Datation carbone 14 des *Cyclope neritea* de la sépulture de la « Dame du Cavillon », *in* de Lumley H. (ed.), *La Grotte du Cavillon, sous la Falaise Des Baousse Rousse Grimaldi, Vintimille, Italie*. CNRS Édition, Paris: 437-440.

Valensi P., Crégut-Bonnoure E. & Defleur A. 2012. — Archeozoological data from the Mousterian level from Moula-Guercy (Ardèche, France) bearing cannibalized Neanderthals remains. *Quaternary International* 252: 48-55. https://doi.org/10.1016/j.quaint.2011.07.028

Verendeev A., Sherwood C. C. & Hopkins W. D. 2016. — Organization and evolution of the neural control of the hand in primates: motor systems, sensory feedback, and laterality, *in* Kivell T. L., Lemelin P., Richmond B. G. & Schmitt D. (eds), *The Evolution of the Primate Hand. Developments in Primatology: Progress and Prospects*. Springer, New York: 131-153. https://doi.org/10.1007/978-1-4939-3646-5_6

Villemeur I. 1992. — Quelques résultats de l'étude morphologique et mécanique de la main des néandertaliens. *Comptes rendus de l'Académie des Sciences. Série 2, Mécanique, Physique, Chimie, Sciences de l'Univers, Sciences de la Terre* 315: 881-884.

VILLEMEUR I. 1994. — *La main des Néandertaliens : comparaison avec la main des hommes de type moderne, morphologie et mécanique*. CNRS Edition (Cahiers de paléoanthropologie), Paris, 178 p.

VLČEK E. 1975. — Morphology of the first metacarpal of Neandertal individuals from the Crimea. *Bulletins et Mémoires de la Société d'Anthropologie de Paris*, Série XIII Tome 2: 257-276.

WILLIAMS-HATALA E. M. 2016. — Biomechanics of the Human hand: from stone tools to computer keyboards, *in* KIVELL T. L., LEMELIN P., RICHMOND B. G. & SCHMITT D. (eds), *The Evolution of the Primate Hand. Developments in Primatology: Progress and Prospects*. Springer, New York: 285-312. https://doi.org/10.1007/978-1-4939-3646-5_11

WILLMES M., GRÜN R., DOUKA K., MICHEL V., ARMSTRONG R. A., BENSON A., CRÉGUT-BONNOURE E., DESCLAUX E., FANG F., KINSLEY L., SAOS T. & DEFLEUR A. 2016. — A comprehensive chronology of the Neanderthal site Moula-Guercy, Ardèche, France. *Journal of Archaeological Science: Reports* 9: 309-319. https://doi.org/10.1016/j.jasrep.2016.08.003

ZHANG Y., NIU J., KELLY-HAYES M., CHAISSON C. E., ALIABADI P., FELSON D. T. 2002. — Prevalence of symptomatic hand osteoarthritis and its impact on functional status among the elderly: the Framingham study. *American Journal of Epidemiology* 156 (11): 1021-1027. https://doi.org/10.1093/aje/kwf141

Submitted on 23 June 2023;
accepted on 26 April 2024;
published on 22 August 2024.

APPENDICES

Appendix 1. — **1**, Raw data in differente sheets: Middle Paleolithic, Upper paleolithic, Cureent Homo sapiens (three previous sheets); **2**, all data about each PCA provide like eignevalue of each principal component, scores of each individual, loading of each variable, etc. Available at: https://doi.org/10.5852/cr-palevol2024v23a21_s1

Appendix 2. — All the data used to establish the linear regression, computed with the Ordinary Least Squares (OLS) algorithm (Hammer & Harper 2023), fit within the normal distributions. See also Appendices 3 and 4. Outliers are few and not far from other data (Appendix 4). Normality: the tests have been made only with the Certosa, Olivier and Teppe Hissar collections as the linear regression has been calculated with these three collections to avoid missing data.

	Maximum length	Morphological length
N	119	119
Shapiro-Wilk W	0.9864	0.9816
p(normal)	0.277	0.1031
Correlation coefficient	0.9944	0.9913

Appendix 3. — Normality of the residuals distribution of the regression line.

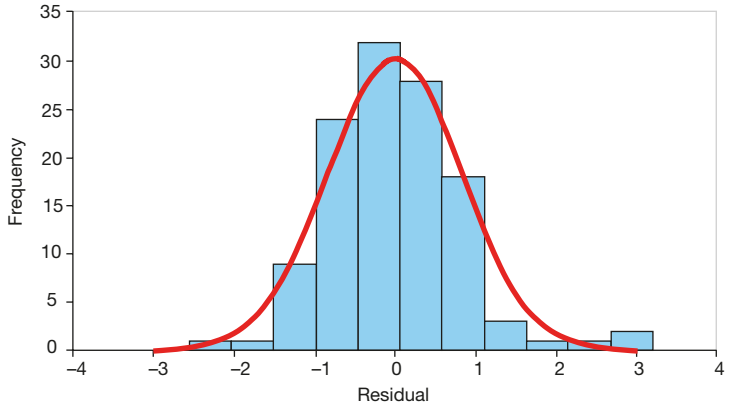

Appendix 4. — Maximum and morphological lengths box plot with outliers (**A**) and regression residual box plot with outliers (**B**).

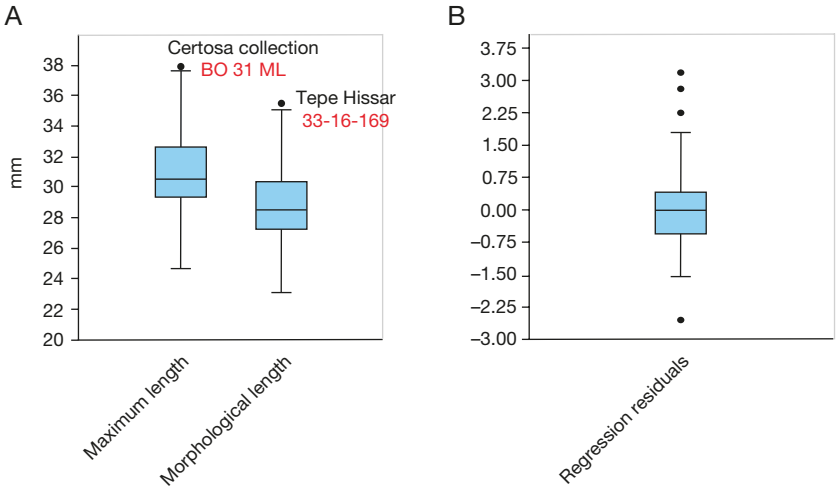

Appendix 5. — Data for inter observers test and calculation details. Available at: https://doi.org/10.5852/cr-palevol2024v23a21_s2

Appendix 6. — Comments on inter-observer error and additional principal component analysis (PCA).

The inter-observer error (see Appendix 5)
Absolute and relative technical error of measurement (TEM) was calculated to quantify observer error. In other words, TEM was calculated to examine variability between multiple observers (inter-observer error) (Perini *et al.* 2005; Langley *et al.* 2018).

Absolute TEM
Absolute TEM is calculated as:

$\sqrt{\frac{\sum_1^N \left[\sum_1^K M(n)^2 - \frac{(\sum_1^K M(n))^2}{K}\right]}{N(K-1)}}$, where N is the sample size, K is the number of observers, M is the measurement, and M(n) is the nth repetition of the measurement.

Relative TEM
Relative TEM is calculated by dividing absolute TEM by the mean and multiplying by 100, and thus it is a measure of precision (or imprecision) unaffected by scale or sample size that allows for the direct comparison of measurements of different scales. Acceptable ranges for the relative, or percent, TEM in anthropometry are <1.5% for intra-examiner error and <2% for inter-examiner error (Langley *et al.* 2018; Perini *et al.* 2005). In our sample, the relative TEM value for all variables is 1.48, so less than 2%.

Principal Component Analysis
The conditions for running the principal component analysis (PCA) are fulfilled, as there are many variables defining each of the factors even if the loadings of each are not so strong (Tabachnick & Fidell 2013). In this case, a sample comprising between 100-200 individuals is enough to get a reliable PCA (Tabachnick & Fidell 2013). Moreover, there are more than five specimens per variable (Tabachnick & Fidell 2013).

Effect of missing data (Appendices 7; 8)
To be sure that missing data do not importantly affect the results we ran a PCA including only complete material (Appendices 1; 7; 8). The result is not significantly different from the PCA including the incomplete remains, because the majority of our sample is complete and very few remains are incomplete.

Effect of side (Appendices 9-11)
The PCAs made with only the left or the right side are not importantly different (Appendices 1; 9-11). In other words, the side does not affect the result of the PCA as the proximal phalanx displays little asymmetry between the two sides (Karakostis *et al.* 2017).

Effect of correlation matrix on the PCA (Appendices 12-14)
All the PCA in this work relies on covariance matrix and thus size could influence the dispersion of the points and the loading of the variables on each of the axes. Thus we have run a PCA relying on a correlation matrix (Appendices 1; 12-14). The loading of some variables on PCA based on correlation matrix diminish because of loss of size effect but the loading distribution of the variables along axes has not changed significantly

Effect of Certosa collection on Neandertal distribution (Appendices 15-17)
In Figure 7 the only modern human sample overlapping completely with Neandertals is the one from Certosa. The same PCA runs without the Certosa collection shows that Neandertal remains are still within modern human samples. The peculiar fitting between the Neandertal and Certosa collection may represent more a coincidence than anything else (Appendices 15-17).

More information about Figure 7
To complete Figure 7 in the main text, the projections on two other planes are also given (Appendices 1; 18; 19), even if, according to the scree plot, the first two PCs are sufficient. In any case, the projection on PC2 and PC3 allows us to see the morphological variation minimizing the effect of size. Neandertal thumb proximal phalanges are not distinguishable from other remains (modern or Upper Paleolithic ones), as numerous authors have already assessed (i.e., Musgrave 1971, 1973, contra Crevecoeur 2014).

Appendix 7. — Effect of missing data. Principal component analysis (PCA) with complete sample. According to the scree plot, the projection on the two first components is enought (**A**, **B**); the projection on the third plane (**C**) is used for the comparaison with the PCA ran with all all data (Figs 7; 8; Appendices 18; 19).

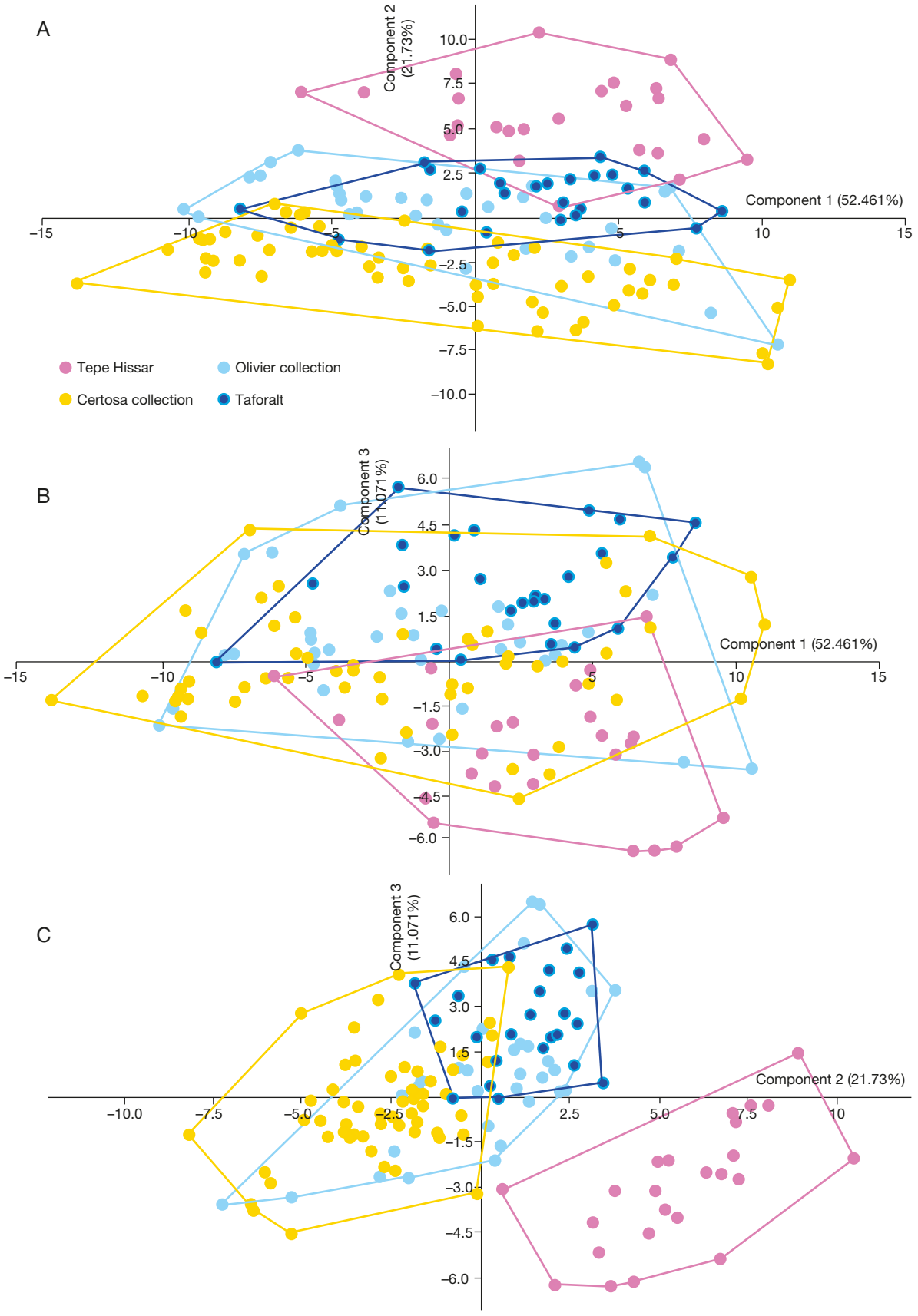

Appendix 8. — Effect of Missing data. Loadings plots of the first three components of the principal component analysis (PCA) runs with samples without no missing data: **A**, PC1; **B**, PC2; **C**, PC3.

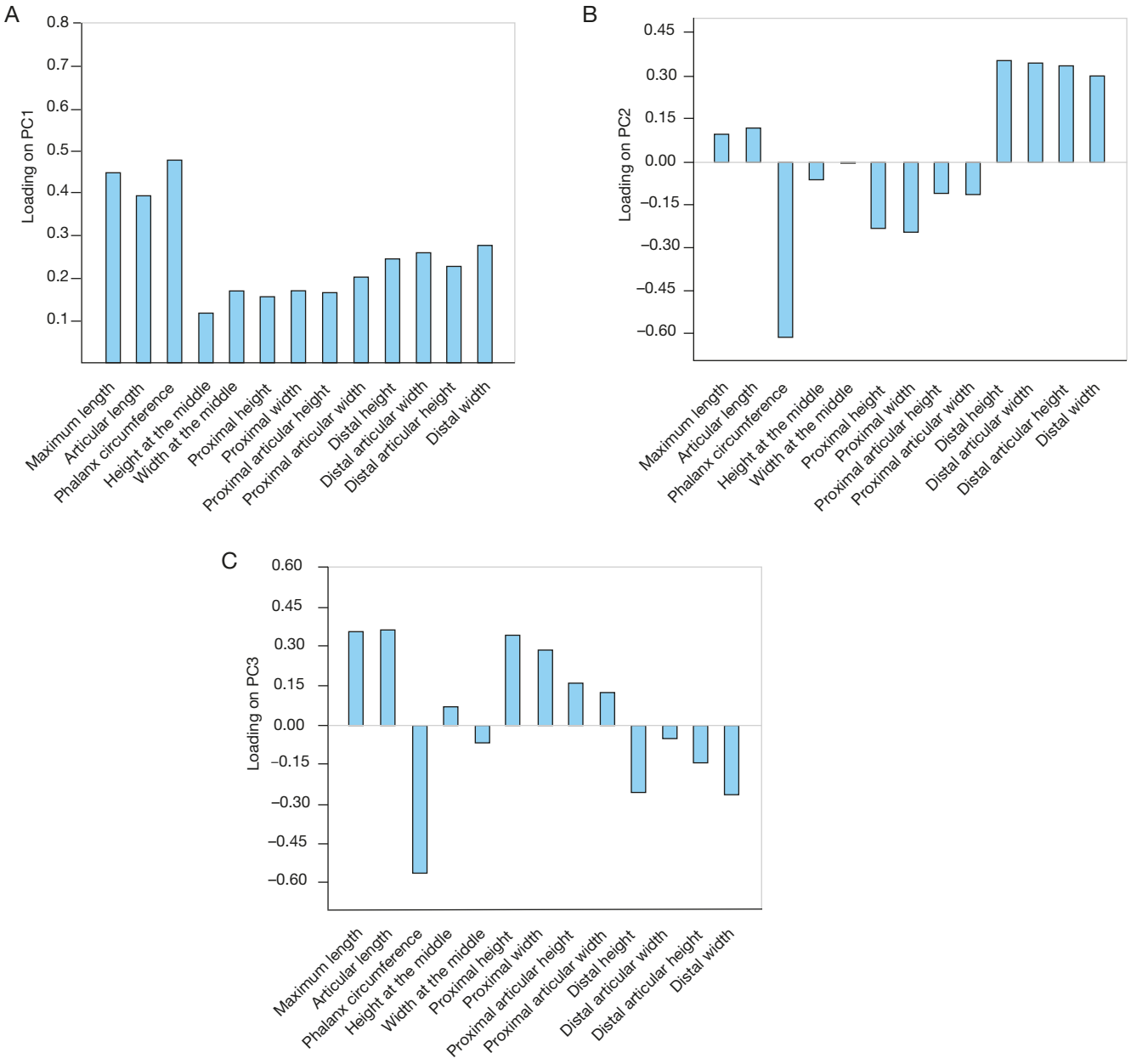

Appendix 9. — Effect of side. Principal component analysis (PCA) with only the right phalanx (**A**) and left one (**B**). According to the scree plot, the projection on the two first components is enough.

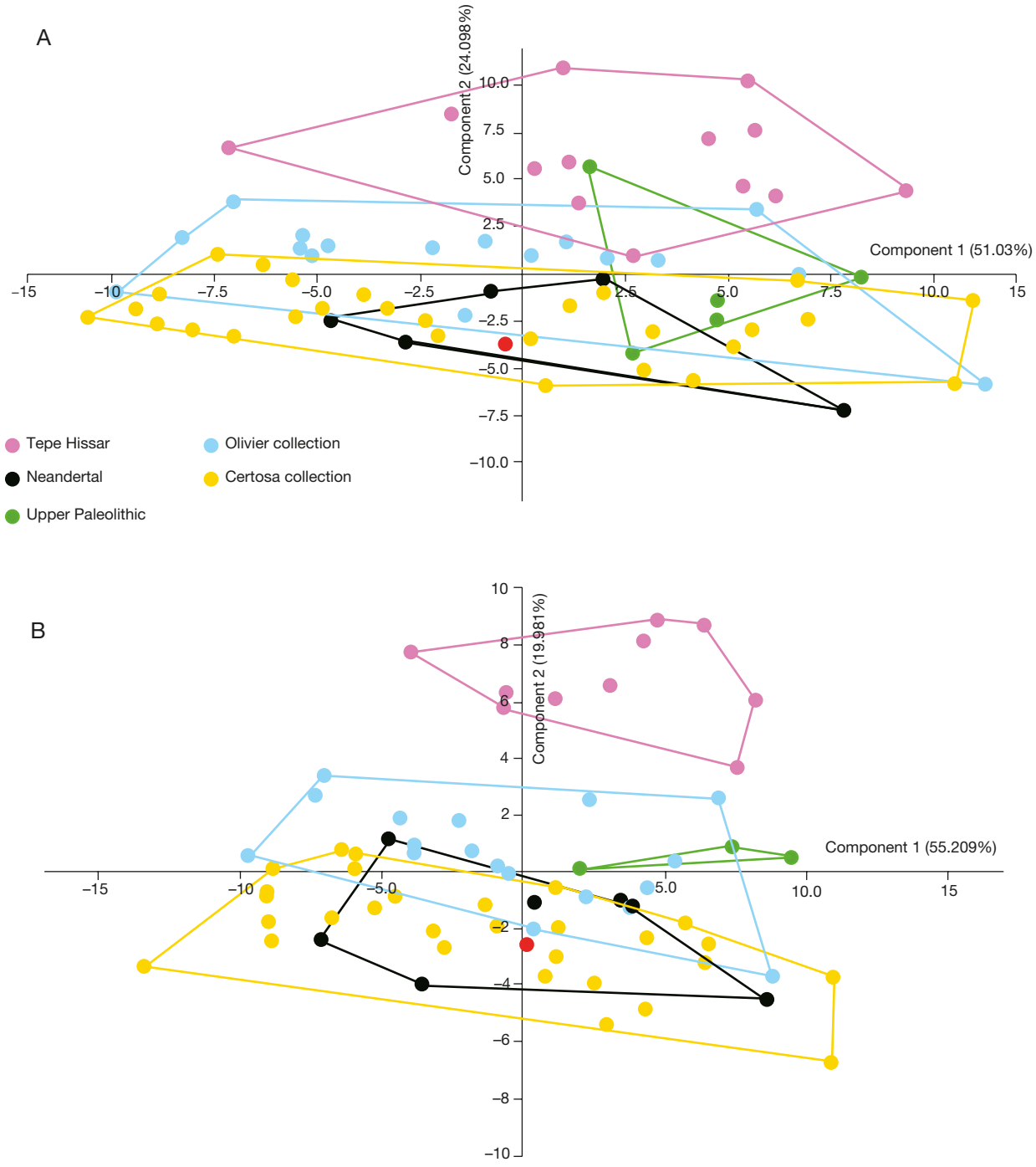

Appendix 10. — Effect of side. Loadings plot of the components 1 (**A**, **B**) and 2 (**C**, **D**) for the two principal component analysis (PCA) (left and right phalanx) and summaries of each PCA: **A**, **C**, left phalanx; **B**, **D**, right phalanx.

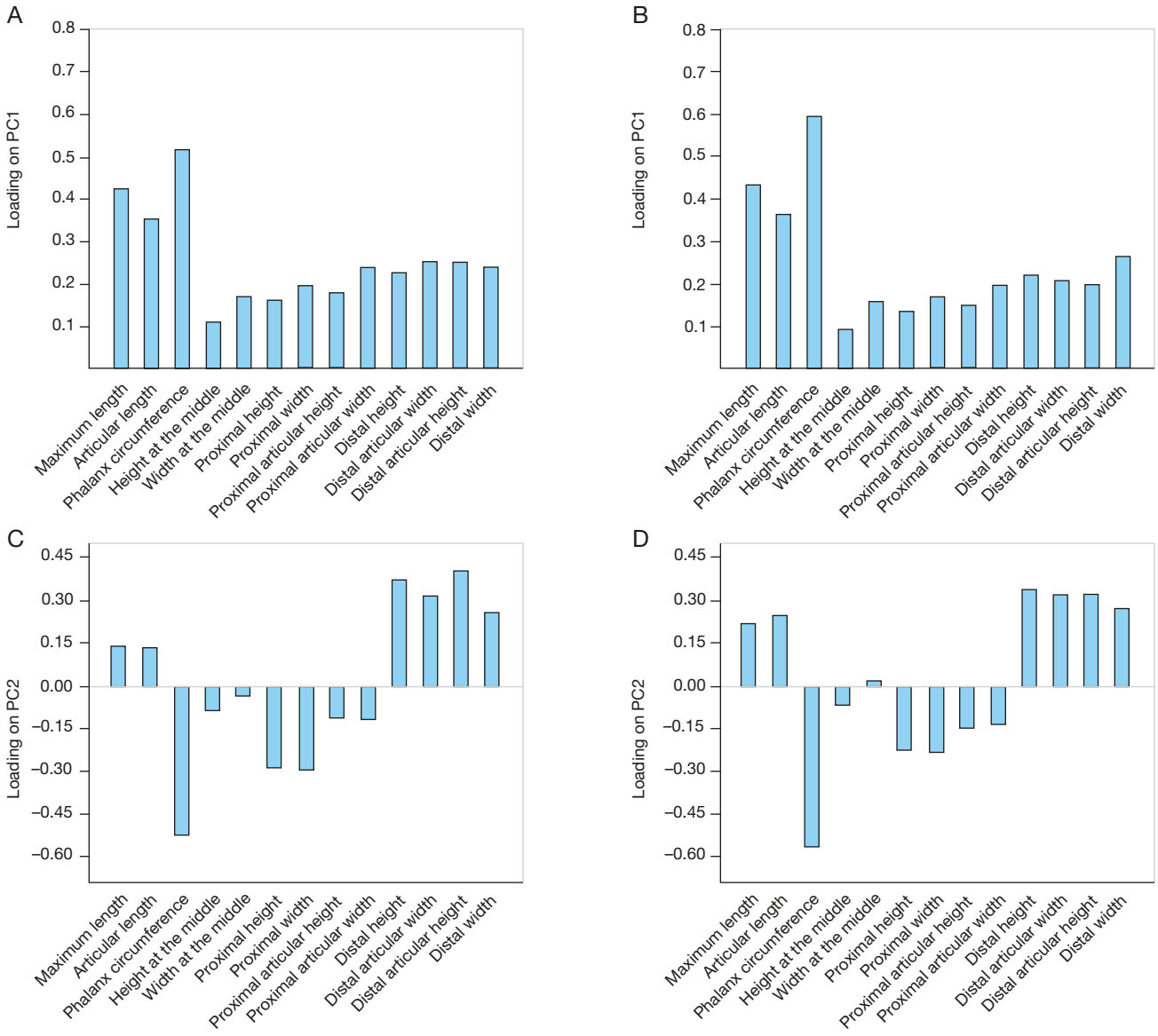

Appendix 11. — Effect of size. Eigenvalue and % of variance of each principal component for the principal component analysis (PCA) in Appendix 9 in relation with Appendix 10. 95% bootstrapped confidence intervals are given for the eigenvalues.

	Right phalanx				Left phalanx			
PC	**Eigenvalue**	**% variance**	**Eig 2.5%**	**Eig 97.5%**	**Eigenvalue**	**% variance**	**Eig 2.5%**	**Eig 97.5%**
1	31.6515	51.03	42.223	59.382	33.4822	55.209	46.429	63.425
2	14.9471	24.098	17.553	31.294	12.1178	19.981	14.02	26.673
3	6.17111	9.9494	6.7118	13.907	6.08755	10.038	6.3323	14.742
4	3.42398	5.5203	3.8085	8.5799	3.36657	5.5511	3.7762	7.5794
5	1.67054	2.6933	1.6391	3.8234	1.50569	2.4827	1.4889	3.2519
6	1.1824	1.9063	0.95893	3.1743	1.2275	2.024	0.88169	3.2418
7	0.750532	1.21	0.63723	1.6624	0.831981	1.3719	0.67207	1.9335
8	0.59495	0.95921	0.48428	1.4252	0.722859	1.1919	0.42694	1.6886
9	0.517497	0.83434	0.2991	1.2457	0.464588	0.76606	0.33208	0.99916
10	0.392805	0.6333	0.25545	0.87672	0.273094	0.4503	0.14255	0.60686
11	0.287262	0.46314	0.15599	0.61684	0.216722	0.35735	0.10698	0.47495
12	0.260499	0.41999	0.1612	0.58572	0.188408	0.31067	0.12489	0.41734
13	0.174817	0.28185	0.1296	0.39907	0.161593	0.26645	0.099571	0.38794

Appendix 12. — Effect of correlation matrix on the PCA. Loading plots of the first two components of the principal component analysis (PCA) runs with a correlation matrix: **A**, PC2; **B**, PC1.

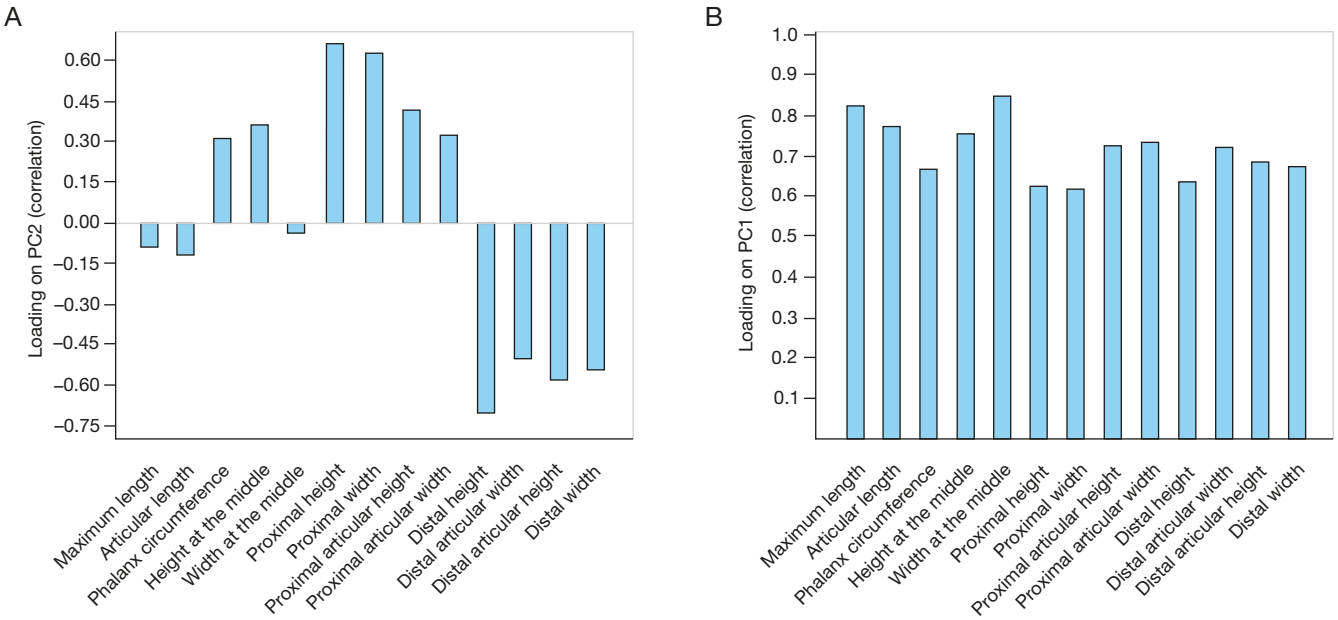

APPENDIX 13. — Effect of correlation matrix on the PCA. Principal component analysis (PCA) with complete sample including projections on the two first components. According to the scree plot, the projection on the two first components is sufficient.

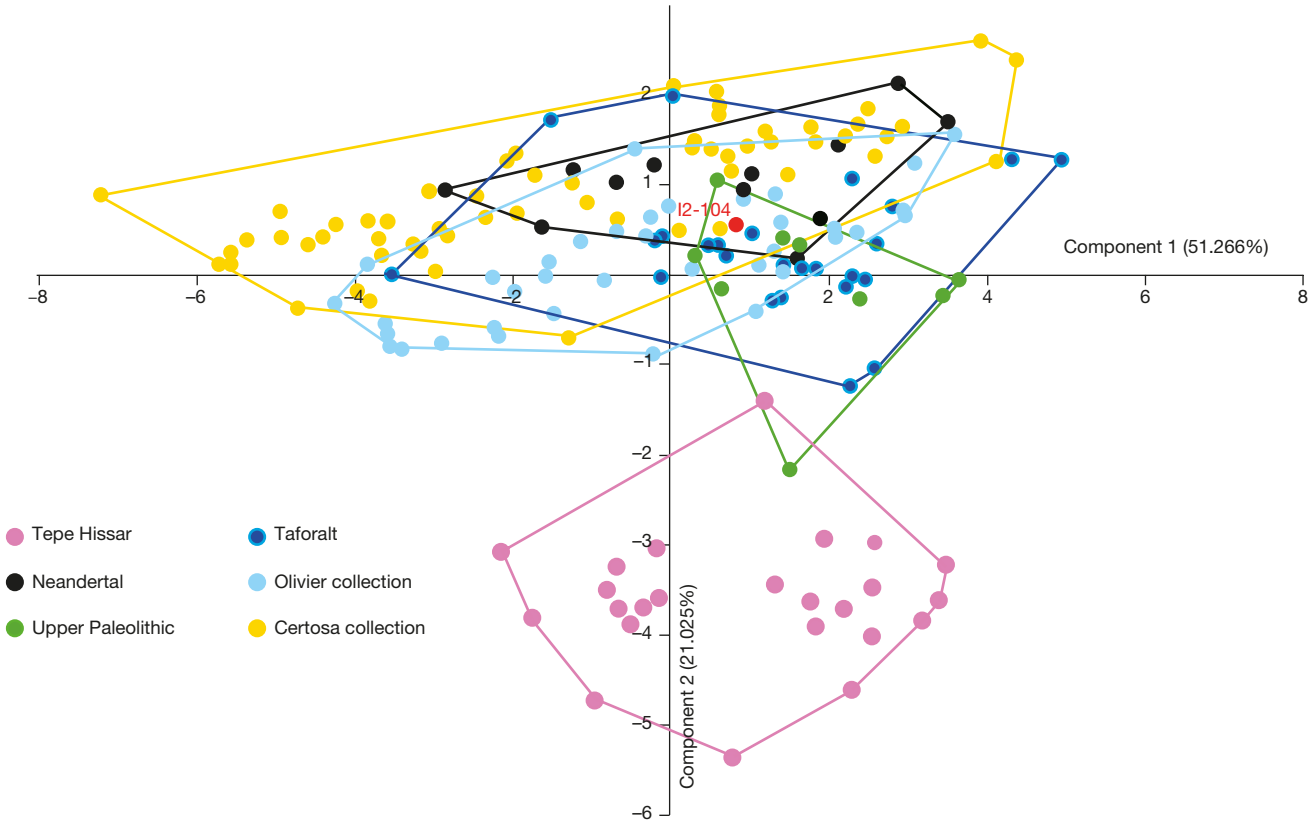

APPENDIX 14. — Effect of correlation matrix. Eigenvalue and % of variance of each principal component for the principal component analysis (PCA) in Appendix 12 in relation with Appendix 13. 95% bootstrapped confidence intervals are given for the eigenvalues.

PC	Eigenvalue	% variance	Eig 2.5%	Eig 97.5%
1	6.43587	49.507	42.617	55.239
2	2.79759	21.52	17.362	26.07
3	0.893377	6.8721	5.4536	8.9983
4	0.69895	5.3765	4.4137	6.5707
5	0.540015	4.154	3.1253	5.6334
6	0.418359	3.2181	2.0902	4.2481
7	0.332899	2.5608	1.4314	3.6229
8	0.287974	2.2152	1.5045	2.859
9	0.204742	1.5749	1.04	2.0161
10	0.159737	1.2287	0.78493	1.53
11	0.113866	0.87589	0.59301	1.0166
12	0.0790682	0.60822	0.36456	0.73359
13	0.03756	0.28892	0.18366	0.35554

Appendix 15. — Effect of Certosa collection on Neandertal distribution. Principal component analysis (PCA) without Certosa collection. According to the scree plot, the projection on the two first components is enough. The projection on the third plane (with PC2 and PC3) is used for the comparison with the PCA ran with all data (Figs 7; 8; Appendices 18; 19).

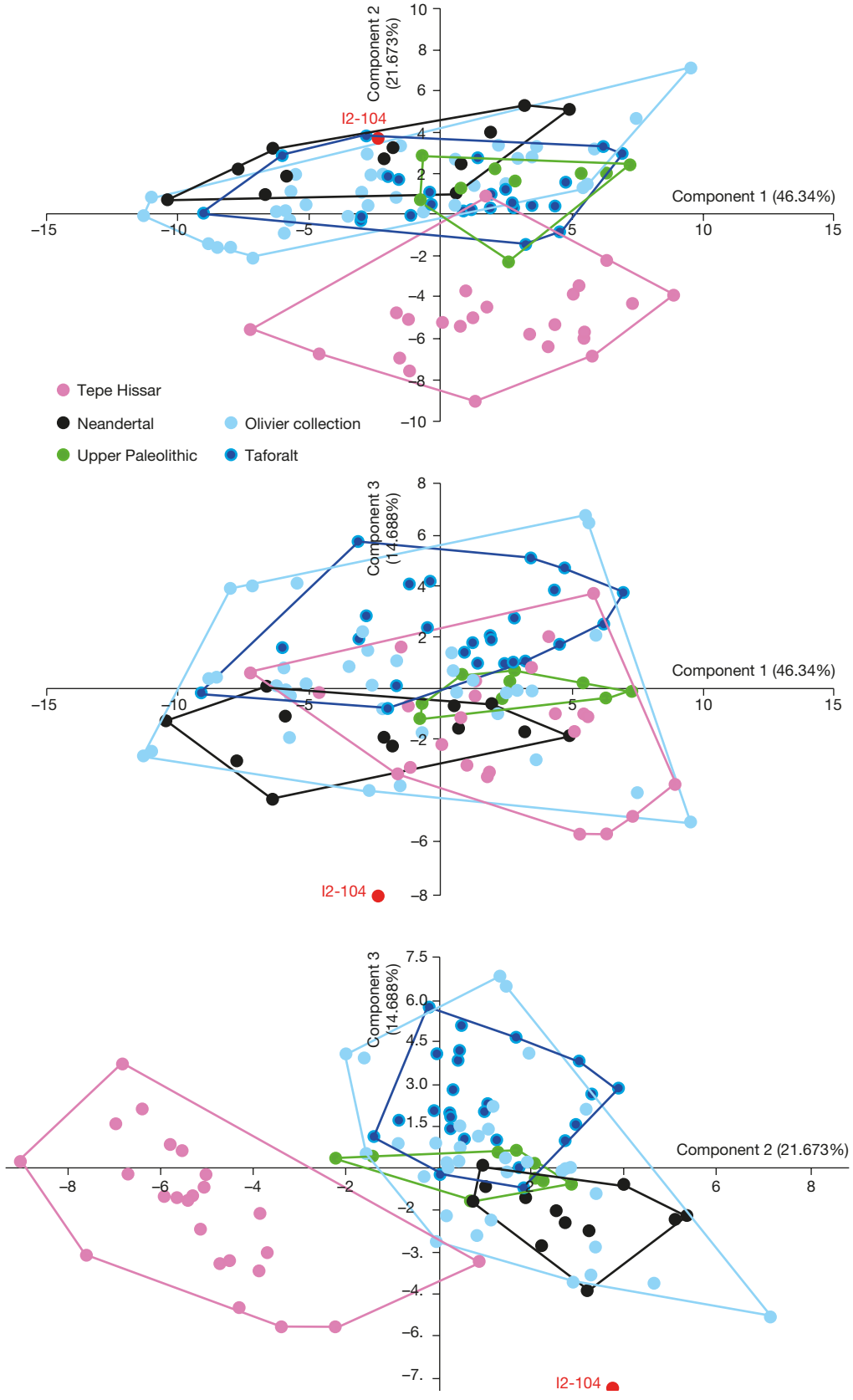

APPENDIX 16. — Effect of Certosa collection on Neandertal distribution. Loading plot for the PC1 (**A**), PC2 (**B**) and PC3 (**C**) and summaries for the principal component analysis (PCA) without Certosa collection.

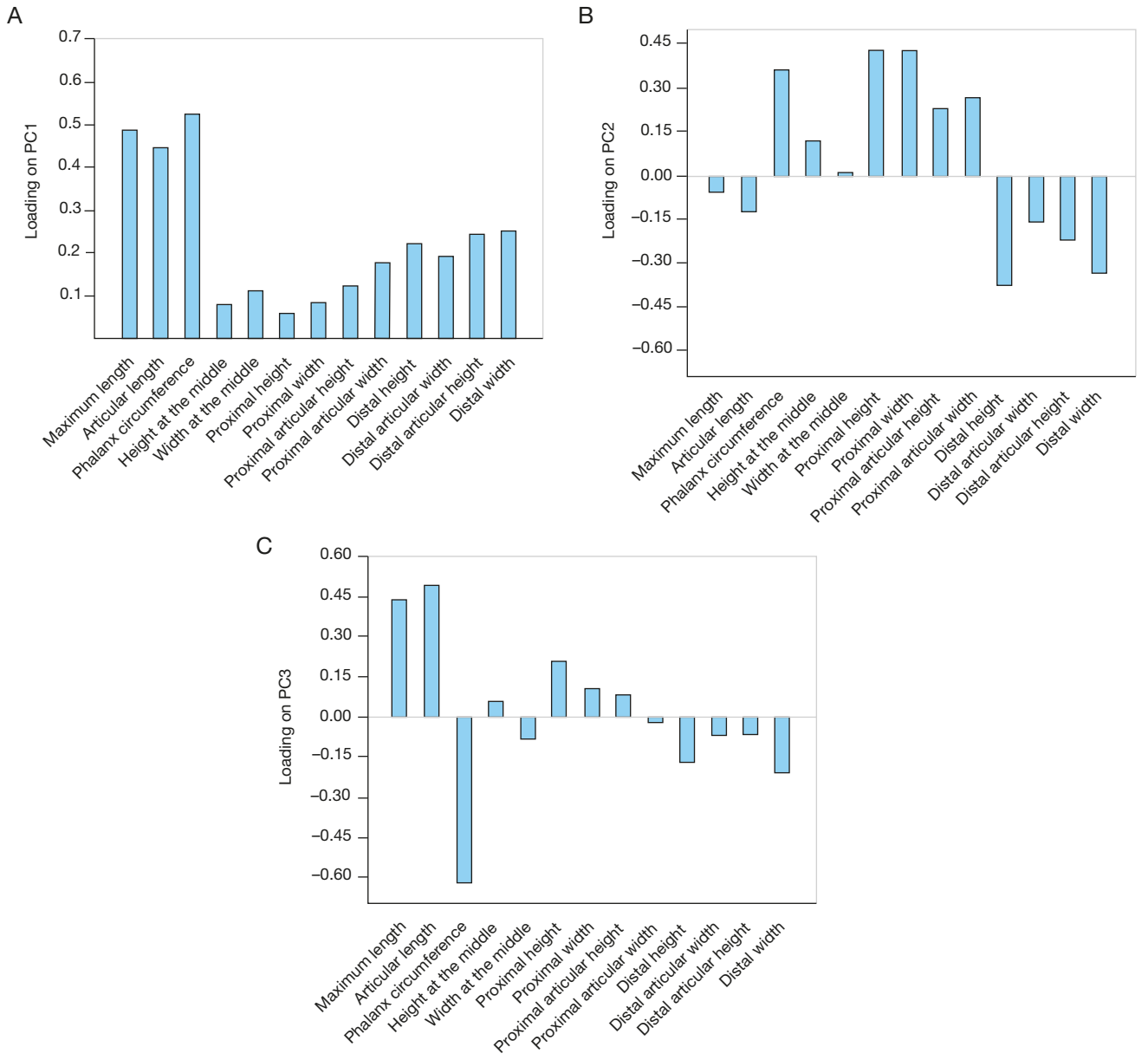

APPENDIX 17. — Effect of Certosa collection on Neandertal distribution. Eigenvalue and % of variance of each principal component for the principal component analysis (PCA) in Appendix 15 in relation with Appendix 16. 95% bootstrapped confidence intervals are given for the eigenvalues.

PC	Eigenvalue	% variance	Eig 2.5%	Eig 97.5%
1	22.6897	46.34	40.252	53.445
2	10.6121	21.673	16.686	26.954
3	7.19195	14.688	10.96	18.367
4	2.57503	5.2591	4.0702	6.6314
5	1.44666	2.9546	2.0073	4.1191
6	1.20416	2.4593	1.1448	3.7288
7	0.995382	2.0329	1.0449	3.0904
8	0.764496	1.5614	0.83003	2.1833
9	0.444535	0.90789	0.48265	1.144
10	0.376836	0.76963	0.42165	1.0325
11	0.281485	0.57489	0.27867	0.70713
12	0.24108	0.49237	0.21613	0.65897
13	0.140119	0.28617	0.15322	0.33217

Appendix 18. — More information about Figure 7 in the main text. Principal component analysis (PCA) projections on PC1 and PC3 as well as on PC 2 and PC 3 representing respectively 62.914% and 31.189% of the total variance: **A**, projection on PC1 and PC3; **B**, projection on PC2 and PC3.

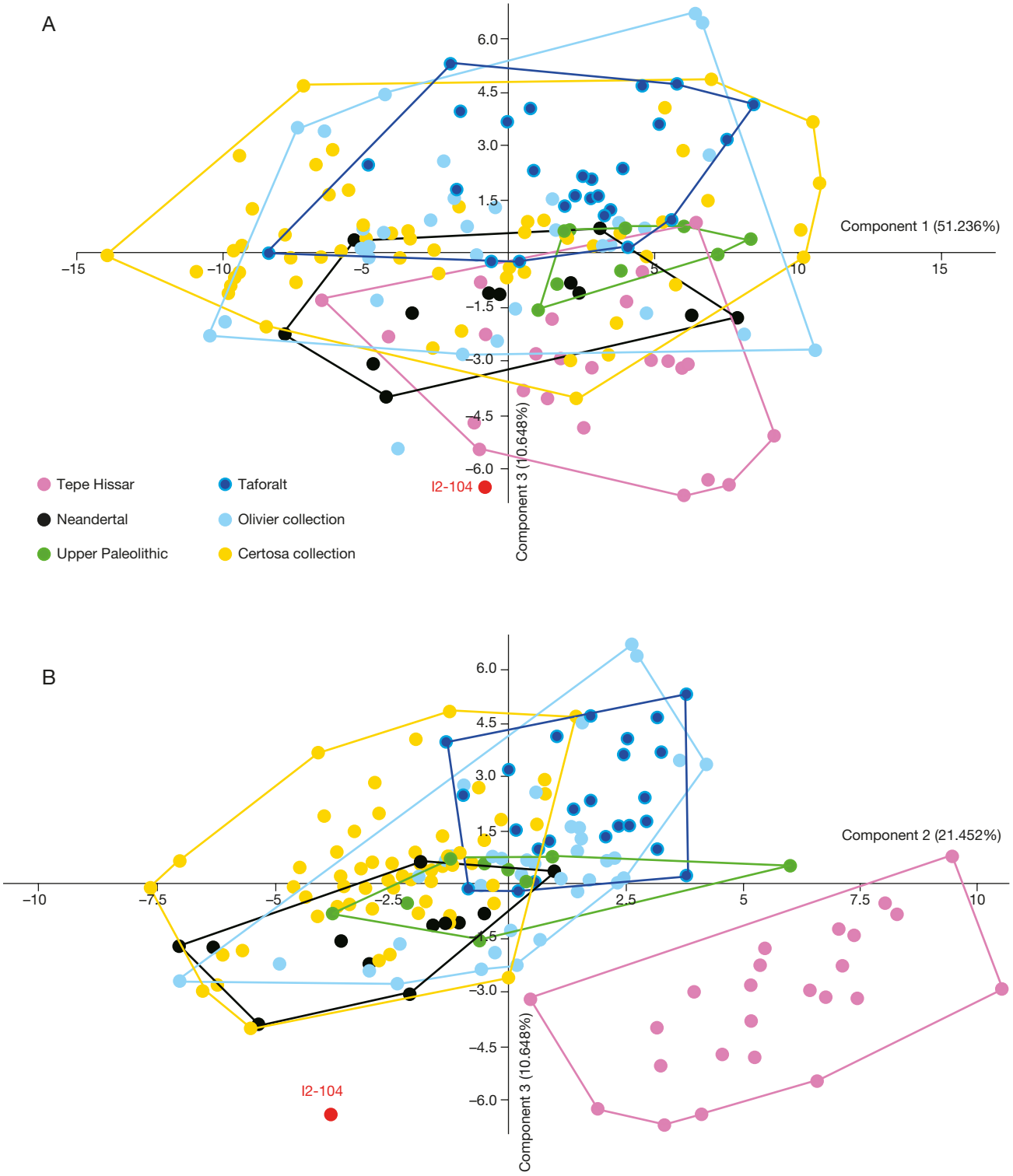

APPENDIX 19. — More information about Figure 7. Loading plot of the PC3 axis (PC1 and PC2 loading plot are in Figure 8)